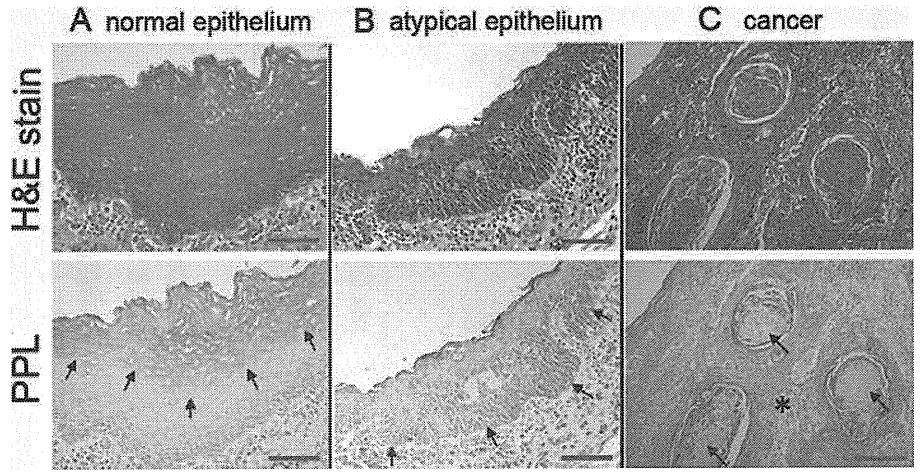

Figure 5 Expression of PPL in normal, atypical epithelium and cancer of the pharyngeal mucosa. (A) In normal hypopharyngeal mucosa, PPL is expressed in the upper layer of the squamous epithelium (arrows). (B) In atypical hypopharyngeal epithelium, PPL expression is rare (arrows). (C) In the pharyngeal cancer epithelium, PPL expression is slight and occurs on the ridge of the cornified epithelium. Note that in both the non-keratinized (asterisk) and keratinized cancer areas (arrows), PPL expression was scarce. Bar: 100 μm.

decreased cellular migration, possibly because of PI3K/Akt axis interference supported by a reduction in phosphorylated Akt at Ser473 (pAktSer473). Collectively, PPL suppression reduced cell motility, and ECM invasion, all of which generate tumor progression by increasing infiltrating activity in pharyngeal squamous cancer cells.

If PPL knockdown reduces cell adhesion activity, PPL may be associated with proliferation and/or cell death because homeostasis in epithelial cells is enforced by their structural characteristics [18,19]. Furthermore, distortion of these balances by PPL siRNA, which interferes with cell adhesion to ECM, is often associated with epithelial tumorigenesis [20]. At this point, attachment to ECM is essential to support cellular functions, including differentiation, apoptosis, proliferation, and migration.

In cancers, the hallmarks of EMT are the acquisition of a migratory and invasive phenotype and/or anoikis resistance, that is, accommodations for survival even in the absence of adhesion to ECM [21,22]. In fibroblast cells, Akt signaling enhances activation of various small guanosine triphosphatases (GTPases), resulting in actin cytoskeleton remodeling and enhanced cell motility [23,24]. In this context, the dephosphorylation of Akt and pAktSer473 induced by PPL siRNA (Figure 4E) is enlightening. LY294002, a PI3K inhibitor, suppressed cellular migration activity in D562 cell (Additional file 5). Since PI3K/Akt/mTOR pathway inhibition is reported to decrease invasion and migration of ovarian carcinoma cell lines [25,26], thus PPL siRNA potentially decreased cellular attachment, migration or movement at least partly via the PI3K/Akt axis.

Moreover, the effects of the matrix are primarily mediated by integrins, a family of cell surface receptors that attach cells to ECM and mediate mechanical and chemical signals from ECM [27]. The PI3K/Akt axis is positively regulated by integrins. Although further studies are necessary, the relationship among PPL, integrins, and the integrin-plectin-vimentin complex potentially bridges ECM and intracellular cytoskeletons [17,28,29]. To investigate the integrins involved in this impaired adhesiveness, a cell adhesion assay using other substrates such as Poly-D/L-lysin, fibronectin, or type-I collagen may be informative. For instance, apoptosis is induced when cells are detached from the surrounding ECM (anoikis) in normal cells [30]. However, cancer or metastatic tumor cells can escape anoikis and thus invade organs (anoikis resistance) [31]. Our results indicate that PPL downregulation is accompanied by PI3K/Akt axis interference which indicates EMT in pharyngeal cancers. In summary, the function of PPL relates to cellular proliferation, cell cycle regulation, cellular movement, and attachment to ECM at least partly via PI3K/Akt axis.

Thus, knockdown of PPL reduced ECM attachment and cellular proliferation. Further studies are required to investigate the role of PPL as a candidate biomarker for diagnosis and treatment of pharyngeal cancers.

Conclusion

The down-regulation of PPL significantly reduced cellular motility and adhesion activity along with phosphorylated AktSer473 suppression. Thus, PPL was positively involved in cellular movement and attachment activity, which was, at least partly achieved via the PI3K/Akt

axis. PPL knockdown is therefore related to reduced cellular movement and attachment activity rather than malignant progression, that is, PPL potentially participates in EMT in pharyngeal cancer cells.

Methods

Patients and tissue samples

Patients with pathologically proven hypopharyngeal squamous cell carcinoma (all primary cases) hospitalized at the Department of Otorhinolaryngology at Chiba University Hospital were investigated in this study. Written informed consent was obtained from each patient prior to surgery.

Cell lines

The D562 pharyngeal cancer cell line was purchased from Human Science Research Resources Bank, Osaka, Japan. TE4, TE9, and TE11 human esophageal cancer cell lines were provided by RIKEN BRC (National Bio-Resource of the MEXT, Tsukuba, Japan) [32,33]. The human esophageal cancer cell lines YES5, TE2, and TTn were kindly provided by Dr. Shimada [34]. All cell lines were cultured at 37°C in a humidified atmosphere containing 5% CO_2 and maintained in IMDM (Iscove's modified Dulbecco's medium; Gibco BRL, NY, USA) in tissue flasks supplemented with 10% heat-inactivated FBS and penicillin (100 units/mL) as well as streptomycin (0.1 mg/mL).

Transient siRNA transfection

Double-stranded siRNA oligonucleotides against PPL and firefly luciferase (GL2), the negative control, were purchased from QIAGEN (Hilden, Germany). Cells were grown to 30-40% confluence in 24-well plates, and 20 pmol of siRNA oligonucleotides was transfected using Lipofectamine 2000 reagent (Invitrogen, Carlsbad, CA, USA). Cells were processed for each assay, and whole-cell proteins were extracted 48-72 h after transfection. Knockdown efficiency of PPL by siRNA was assessed by immunoblotting.

Immunoblotting

Cells were dissolved in lysis buffer (7 M urea, 2 M thiourea, 2% 3-[(3-cholamidopropyl)dimethylammonio-] 1-propanesulfate, 0.1 M dithiothreitol, 2% IPG buffer (GE Healthcare, Buckinghampshire, UK), and 40 mM Tris) using a Polytron homogenizer (Kinematica, Switzerland) following centrifugation (100,000 × *g*) for 1 h at 4°C. The amount of protein in the supernatant was measured by protein assay (Bio-Rad, Hercules, CA, USA). The proteins were separated by electrophoresis on 7.5% polyacrylamide gels and transferred to a polyvinylidene fluoride membrane (Millipore, Bedford, MA, USA) in a tank transfer apparatus (Bio-Rad, Hercules, CA, USA). The membrane was blocked with 0.5% skim milk in phosphate-buffered saline (PBS) or 0.5% bovine serum albumin (BSA) in tris-buffered saline with Tween 20 (TBST) for 1 h, and probed with a primary antibody diluted in blocking buffer. Anti-PPL (Betyl Laboratory Ltd., Montgomery, TX, USA), anti-phospho-AKT (Ser473 or Thr308), anti-phospho-MAPK (Cell Signaling Technology, Beverly, MA, USA), and anti-β-actin (Santa Cruz, CA, USA) were used as primary antibodies. Donkey anti-rabbit IgG horseradish peroxidase (HRP) conjugate (Amersham Pharmacia Biotech, Piscataway, NJ, USA) diluted 1:3,000 and rabbit anti-goat IgG HRP (Cappel, West Chester, PA, USA) diluted 1:500 were used as secondary antibodies. Antigens on the membrane were detected by ECL™ detection reagents (GE Healthcare, Buckinghamshire, UK).

Proliferation assay

Five thousand cells were seeded in 24-well Falcon 3072 plates (Becton Dickinson, Lincoln Park, NJ, USA) at 37° C and 5% CO_2. After various periods, cell number was established by counting with a phase-contrast Leitz microscope (MD, USA).

Flow cytometry

For cell cycle analysis, 1×10^6 cells were seeded in 10-cm-diameter culture dishes. Cells were trypsinized, washed with ice-cold PBS, fixed in 70% ethanol, and stored at -20°C. The cells were then treated with RNase (0.2 mg/mL) for 0.5 h at 37°C and stained with propidium iodide at 50 μg/mL. The stained cells were analyzed in a FACSCalibur cytometer (Becton Dickinson, Lincoln Park, NJ, USA), and the results were analyzed with FlowJo software (Tree Star Inc., San Carlos, CA, USA).

BrdU incorporation assay

The BrdU incorporation assay was carried out as described previously, using the BrDu flow kit (Becton Dickinson, Lincoln Park, NJ, USA) according to the manufacturer's instructions [35]. In brief, $1\text{-}2 \times 10^6$ cells were labeled with 10 μM BrdU for 1 h, harvested, fixed, and treated with DNAase. Cells were stained with anti-BrdU FITC-coupled antibody and 7-AAD for DNA. Samples were analyzed in a FACSCalibur cytometer (Becton Dickinson, Lincoln Park, NJ, USA) using the FlowJo program (Ashland, OR, USA). BrdU signals were recorded on a logarithmic scale in the FL1 channel, and DNA was recorded on a linear scale in the FL3 channel. Single cell events were distinguished from cell aggregates on a FL3-A versus FL3-W plot of 7-AAD fluorescence.

Wound-healing assay

Cells were transfected with PPL siRNA or pretreated for 2 h with PI3K inhibitor, LY294002 (Wako, Osaka,

Japan). Then, cells were grown to confluence in 6-well plates, and monolayer cells were scraped using a micropipette (yellow) tip. After washing with PBS, serum-free medium was added to prevent cell proliferation. Photographs of the wounded area were taken immediately after the scratch was made. Six and 24 h after scraping, cell movement into the wounded area was monitored by time-lapse microscopy.

Adhesion assay

Adhesion of PC-3 cells was measured as described previously, with some modifications [36,37]. In brief, each well of a 24-well plate was coated with 200 μg/ml Matrigel (Becton Dickinson, Lincoln Park, NJ, USA). In each well, 2×10^4 cells were added in 0.5 mL serum-free media supplemented with 0.1% BSA. The plates were incubated at 37°C and adhesion was determined at 0.5 h. The plates were fixed with methanol and stained with Diff-Quik (Sysmex Corp., Kobe, Japan). The number of cells adhered to the Matrigel was counted at 4 random fields per well in duplicate at a magnification of ×400.

Time-lapse microscopy

Time-lapse recordings of cells were made with an Axiovert 200 M SP LSM 510 META confocal laser scanning microscope (Carl Zeiss Inc., Oberkechen, Germany) equipped with an AxioCam charge-coupled device (CCD) camera (Zeiss, Germany) and AxioVision software. Cells were maintained in an environmental chamber at 37°C with 5% CO_2 during the analysis. Images were taken by CCD camera through a laser scanning microscope every 5 min. Cell tracking was performed using AxioVision software. Images were imported into Adobe Photoshop and prepared as pictures.

Immunohistochemical staining

Immunohistochemical procedures for PPL expression have been described previously [38]. In brief, air-dried 4-micron cryostat sections were fixed in cold acetone for 20 min and washed with PBS for 5 min. The sections were then incubated with anti-PPL antibody overnight at 4°C. After washing with PBS, the sections were incubated with biotinylated anti-rabbit IgG as a secondary antibody. The sections were then incubated with HRP-conjugated streptavidin-biotin complex for 0.5 h. Peroxidase activity was visualized by DAB solution (20 mg of 3,3'-diaminobenzidine, 65 mg of sodium azide, and 10 mL of 30% hydrogen peroxide in 100 mL of 0.05 M Tris buffer at pH 7.6). Hematoxylin was used for nuclear counterstaining.

Statistical Analysis

The abovementioned experiments were repeated at least 3 times. Student's t-test was used for statistical analysis.

Additional material

Additional file 1: Adhesion assay of D562 cells.

Additional file 2: siRNA against PPL reduces adhesion to ECM in D562 cells. D562 cells were transfected with either control siRNA (Additional file 1) or PPL siRNA (Additional file 2). The cells were grown to confluence in glass-bottomed dishes and EDTA (2.5 mM final concentration) was added. Images were analyzed by time-lapse confocal laser scanning microscopy using a laser-scanning confocal microscope (LSM 510 META; Carl Zeiss Inc). Frames were taken every 5 min for 6 h.

Additional file 3: Migration of D562 cells.

Additional file 4: siRNA against PPL reduces cell migration in D562 cells. D562 cells were transfected with either control siRNA (Additional file 3) or PPL siRNA (Additional file 4). After 24 h, cells were seeded on glass-bottomed dishes and incubated for another 24 h. Images were analyzed by time-lapse confocal laser scanning microscopy using a laser-scanning confocal microscope. Frames were taken every 5 min for 24 h.

Additional file 5: pAktSer473 phosphorylation affects cellular movement in D562 cells. (A) (B) 5×10^5 YES5 cells (low PPL expression) and D562 cells (high PPL expression) were injected beneath right thigh of 8-week male nude mice and monitored subsequent tumor growth. No tumor growth was observed in YES5 mice, while some tumors were observed in D562 mice. (C) LY294002, a PI3K inhibitor, suppressed pAktSer473 phosphorylation but did not alter PPL expressio in D562 cells. (D) LY294002 suppressed D562 cell migration revealed by wound-healing assay in D562 cells. (E) The ratio of width at 6 hrs/0 hr (%) indicated that LY294002 suppressed wound-healing in D562 cells.

Abbreviations

PPL: periplakin; siRNAs: short interfering RNAs; PKB: protein kinase B; EMT: epithelial-mesenchymal transition; ECM: extracellular matrix; PI3K: phosphatidylinositol 3' kinase.

Acknowledgements

The authors thank Ms. Mai Tamura for technical assistance.

Author details

[1]Department of Otorhinolaryngology, Chiba University Hospital, 1-8-1 Inohana, Chiba City, Chiba 260-8670, Japan. [2]Department of Molecular Diagnosis, Graduate School of Medicine, Chiba University Hospital, 1-8-1 Inohana, Chiba City, Chiba 260-8670, Japan. [3]Department of Clinical Proteomics Research Center, Chiba University Hospital, 1-8-1 Inohana, Chiba City, Chiba 260-8670, Japan. [4]Proteome Research Center, Proteome Research Project, National Institute of Biomedical Innovation, 7-6-8 Saito-Asagi, Ibaraki City, Osaka 567-0085, Japan. [5]Department of General and Gastrointestinal Surgery, Toho University Omori Medical Center, 6-11-1 Ohta-ku, Ohmorinishi, Tokyo 143-8541, Japan. [6]Department of Diagnostic Pathology, Graduate School of Medicine, Chiba University, 1-8-1 Inohana, Chiba City, Chiba 260-8670, Japan.

Authors' contributions

YT performed all experiments. YT and KM designed the experiment and prepared the manuscript. TT, KK, NT, HS, FN and YO contributed scientific and financial support. FN is responsible for the entire study. All the authors have read and approved the final manuscript.

Competing interests

The authors declare that they have no competing interests.

Received: 26 January 2011 Accepted: 27 September 2011
Published: 27 September 2011

References

1. Daly JM, Karnell LH, Menck HR: **National Cancer Data Base report on esophageal carcinoma.** *Cancer* 1996, **78**:1820-8.
2. Nishimori T, Tomonaga T, Matsushita K, Oh-Ishi M, Kodera Y, Maeda T, Nomura F, Matsubara H, Shimada H, Ochiai T: **Proteomic analysis of**

primary esophageal squamous cell carcinoma reveals downregulation of a cell adhesion protein, periplakin. *Proteomics* 2006, **6**:1011-8.
3. Hatakeyama H, Kondo T, Fujii K, Nakanishi Y, Kato H, Fukuda S, Hirohashi S: **Protein clusters associated with carcinogenesis, histological differentiation and nodal metastasis in esophageal cancer.** *Proteomics* 2006, **6**:6300-16.
4. Sonnenberg A, Liem RK: **Plakins in development and disease.** *Exp Cell Res* 2007, **313**:2189-203.
5. Lunter PC, Wiche G: **Direct binding of plectin to Fer kinase and negative regulation of its catalytic activity.** *Biochem Biophys Res Commun* 2002, **296**:904-10.
6. Gregor M, Zeold A, Oehler S, Marobela KA, Fuchs P, Weigel G, Hardie DG, Wiche G: **Plectin scaffolds recruit energy-controlling AMP-activated protein kinase (AMPK) in differentiated myofibres.** *J Cell Sci* 2006, **119**:1864-75.
7. van den Heuvel AP, de Vries-Smits AM, van Weeren PC, Dijkers PF, de Bruyn KM, Riedl JA, Burgering BM: **Binding of protein kinase B to the plakin family member periplakin.** *J Cell Sci* 2002, **115**:3957-66.
8. Larue L, Bellacosa A: **Epithelial-mesenchymal transition in development and cancer: role of phosphatidylinositol 3' kinase/AKT pathways.** *Oncogene* 2005, **24**:7443-54.
9. Hunton DL, Barnes WG, Kim J, Ren XR, Violin JD, Reiter E, Milligan G, Patel DD, Lefkowitz RJ: **Beta-arrestin 2-dependent angiotensin II type 1A receptor-mediated pathway of chemotaxis.** *Mol Pharmacol* 2005, **67**:1229-36.
10. Naga Prasad SV, Jayatilleke A, Madamanchi A, Rockman HA: **Protein kinase activity of phosphoinositide 3-kinase regulates beta-adrenergic receptor endocytosis.** *Nat Cell Biol* 2005, **7**:785-96.
11. Sun Y, Cheng Z, Ma L, Pei G: **Beta-arrestin2 is critically involved in CXCR4-mediated chemotaxis, and this is mediated by its enhancement of p38 MAPK activation.** *J Biol Chem* 2002, **277**:49212-9.
12. Francke F, Ward RJ, Jenkins L, Kellett E, Richter D, Milligan G, Bachner D: **Interaction of neurochondrin with the melanin-concentrating hormone receptor 1 interferes with G protein-coupled signal transduction but not agonist-mediated internalization.** *J Biol Chem* 2006, **281**:32496-507.
13. Murdoch H, Feng GJ, Bachner D, Ormiston L, White JH, Richter D, Milligan G: **Periplakin interferes with G protein activation by the melanin-concentrating hormone receptor-1 by binding to the proximal segment of the receptor C-terminal tail.** *J Biol Chem* 2005, **280**:8208-20.
14. Ward RJ, Jenkins L, Milligan G: **Selectivity and functional consequences of interactions of family A G protein-coupled receptors with neurochondrin and periplakin.** *J Neurochem* 2009, **109**:182-92.
15. Boczonadi V, McInroy L, Maatta A: **Cytolinker cross-talk: periplakin N-terminus interacts with plectin to regulate keratin organisation and epithelial migration.** *Exp Cell Res* 2007, **313**:3579-91.
16. Long HA, Boczonadi V, McInroy L, Goldberg M, Maatta A: **Periplakin-dependent re-organisation of keratin cytoskeleton and loss of collective migration in keratin-8-downregulated epithelial sheets.** *J Cell Sci* 2006, **119**:5147-59.
17. Hong KO, Kim JH, Hong JS, Yoon HJ, Lee JI, Hong SP, Hong SD: **Inhibition of Akt activity induces the mesenchymal-to-epithelial reverting transition with restoring E-cadherin expression in KB and KOSCC-25B oral squamous cell carcinoma cells.** *J Exp Clin Cancer Res* 2009, **28**:28-38.
18. Hanahan D, Weinberg RA: **The hallmarks of cancer.** *Cell* 2000, **100**:57-70.
19. Perez-Moreno M, Jamora C, Fuchs E: **Sticky business: orchestrating cellular signals at adherens junctions.** *Cell* 2003, **112**:535-48.
20. Silva JM, Ezhkova E, Silva J, Heart S, Castillo M, Campos Y, Castro V, Bonilla F, C : **Cyfip1 is a putative invasion suppressor in epithelial cancers.** *Cell* 2009, **137**:1047-61.
21. Daouti S, Li WH, Qian H, Huang KS, Holmgren J, Levin W, Reik L, McGady DL, Gillespie P, Perrotta A, Bian H, Reidhaar-Olson JF, Bliss AR, Olivier JA, Sergi D, Fry W, Danho S, Ritland N, Fotouhi SA, Heimbrook D, Niu H: **A selective phosphatase of regenerating liver phosphatase inhibitor suppresses tumor cell anchorage-independent growth by a novel mechanism involving p130Cas cleavage.** *Cancer Res* 2008, **68**:1162-9.
22. Guarino M, Rubino B, Ballabio G: **The role of epithelial-mesenchymal transition in cancer pathology.** *Pathology* 2007, **39**:305-18.
23. Enomoto A, Murakami H, Asai N, Morone N, Watanabe T, Kawai K, Murakumo Y, Usukura J, Kaibuchi K, Takahashi M: **Akt/PKB regulates actin organization and cell motility via Girdin/APE.** *Dev Cell* 2005, **9**:389-402.
24. Enomoto A, Ping J, Takahashi M: **Girdin, a novel actin-binding protein, and its family of proteins possess versatile functions in the Akt and Wnt signaling pathways.** *Ann N Y Acad Sci* 2006, **1086**:169-84.
25. Kim EK, Yun SJ, Ha JM, Kim YW, Jin IH, Yun J, Shin HK, Song SH, Kim JH, Lee JS, Kim CD, Bae SS: **Selective activation of Akt1 by mammalian target of rapamycin complex 2 regulates cancer cell migration, invasion, and metastasis.** *Oncogene* 2011, **30**:2954-63.
26. Karam AK, Santiskulvong C, Fekete M, Zabih S, Eng C, Dorigo O: **Cisplatin and PI3kinase inhibition decrease invasion and migration of human ovarian carcinoma cells and regulate matrix-metalloproteinase expression.** *Cytoskeleton* 2010, **67**:535-544.
27. Giancotti FG, Ruoslahti E: **Integrin signaling.** *Science* 1999, **285**:1028-32.
28. Bhattacharya R, Gonzalez AM, Debiase PJ, Trejo HE, Goldman RD, Flitney FW, Jones JC: **Recruitment of vimentin to the cell surface by beta3 integrin and plectin mediates adhesion strength.** *J Cell Sci* 2009, **122**:1390-400.
29. Kazerounian S, Uitto J, Aho S: **Unique role for the periplakin tail in intermediate filament association: specific binding to keratin 8 and vimentin.** *Exp Dermatol* 2002, **11**:428-38.
30. Jinka R, Kapoor R, Pavuluri S, Thatipalli AR, Jerald MK, Rao L, Pande G: **Differential gene expression and clonal selection during cellular transformation induced by adhesion deprivation.** *BMC Cell Biol* 2010, **11**:93-104.
31. Barnes EA, Kenerson HL, Jiang X, Yeung RS: **Tuberin regulates E-cadherin localization: implications in epithelial-mesenchymal transition.** *Am J Pathol* 2010, **177**:1765-78.
32. Jia LQ, Osada M, Ishioka C, Gamo M, Ikawa S, Suzuki T, Shimodaira H, Niitani T, Kudo T, Akiyama M, Kimura N, Matsuo M, Mizusawa H, Tanaka N, Namba M, Kanamaru R, Kuroki T: **Screening the p53 status of human cell lines using a yeast functional assay.** *Mol Carcinog* 1997, **19**:243-53.
33. Kajimoto T, Shirai Y, Sakai N, Yamamoto T, Matsuzaki H, Kikkawa U, Saito N: **Ceramide-induced apoptosis by translocation, phosphorylation, and activation of protein kinase Cdelta in the Golgi complex.** *J Biol Chem* 2004, **279**:12668-76.
34. Iizuka N, Miyamoto K, Okita K, Tangoku A, Hayashi H, Yosino S, Abe T, Morioka T, Hazama S, Oka M: **Inhibitory effect of Coptidis Rhizoma and berberine on the proliferation of human esophageal cancer cell lines.** *Cancer Lett* 2000, **148**:19-25.
35. Cheng A, Solomon MJ: **Speedy/Ringo C regulates S and G2 phase progression in human cells.** *Cell Cycle* 2008, **7**:3037-47.
36. Pelayo BA, Fu YM, Meadows GG: **Decreased tissue plasminogen activator and increased plasminogen activator inhibitors and increased activator protein-1 and specific promoter 1 are associated with inhibition of invasion in human A375 melanoma deprived of tyrosine and phenylalanine.** *Int J Oncol* 2001, **18**:877-83.
37. Uhlenkott CE, Huijzer JC, Cardeiro DJ, Elstad CA, Meadows GG: **Attachment, invasion, chemotaxis, and proteinase expression of B16-BL6 melanoma cells exhibiting a low metastatic phenotype after exposure to dietary restriction of tyrosine and phenylalanine.** *Clin Exp Metastasis* 1996, **14**:125-37.
38. Matsushita K, Tomonaga T, Shimada H, Shioya A, Higashi M, Matsubara H, Harigaya K, Nomura F, Libutti D, Levens D, Ochiai T: **An essential role of alternative splicing of c-myc suppressor FUSE-binding protein-interacting repressor in carcinogenesis.** *Cancer Res* 2006, **66**:1409-17.

doi:10.1186/1471-2121-12-41
Cite this article as: Tonoike *et al.*: Adhesion molecule periplakin is involved in cellular movement and attachment in pharyngeal squamous cancer cells. *BMC Cell Biology* 2011 **12**:41.

JOURNAL OF PROTEOMICS 74 (2011) 858–873

available at www.sciencedirect.com

ScienceDirect

www.elsevier.com/locate/jprot

Global expression study in colorectal cancer on proteins with alkaline isoelectric point by two-dimensional difference gel electrophoresis

Taika Muto[a,b], *Hirokazu Taniguchi*[c], *Ryoji Kushima*[c], *Hitoshi Tsuda*[c], *Hirotaka Yonemori*[a], *Chen Chen*[a], *Yutaka Sugihara*[a], *Kano Sakamoto*[a], *Yukiko Kobori*[a], *Helen Palmer*[a,1], *Yukiko Nakamura*[a,d], *Takeshi Tomonaga*[d], *Hiroshi Tanaka*[b,e], *Hiroshi Mizushima*[e], *Shin Fujita*[f], *Tadashi Kondo*[a,*]

[a]*Division of Pharmacoproteomics, National Cancer Center Research Institute, Japan*
[b]*Bioinformatics Laboratory, Graduate School of Medical and Dental Sciences, Tokyo Medical Dental University, Japan*
[c]*Division of Pathology, National Cancer Center Hospital, Japan*
[d]*Laboratory of Proteome Research, National Institute of Biomedical Innovation, Japan*
[e]*Department for Medical Omics Informatics, School of Biomedical Science, Tokyo Medical and Dental University, Japan*
[f]*Colorectal Surgery Division, National Cancer Center Hospital, Japan*

ARTICLE INFO

Article history:
Received 2 February 2011
Accepted 26 February 2011
Available online 6 March 2011

ABSTRACT

Colorectal cancer is one of the leading causes of cancer death worldwide. To identify candidates for biomarkers and therapeutic targets, we investigated the proteome of colorectal cancer tissues. Using 2D-DIGE in combination with our original large format electrophoresis apparatus, we compared surgically resected normal and tumor tissues from 53 patients with colorectal cancer. We focused on proteins with an alkaline pI using IPG gels for the alkaline range. We observed 1687 protein spots, and found 100 spots with statistical ($p<0.01$) and significant (>2-fold) differences between the normal and the tumor tissue groups. Among these 100 protein spots, five showed a different intensity between tumor tissues from the stage-II and the stage-III patients. MS experiments revealed that these 100 protein spots corresponded to 58 unique proteins. These included six proteins which had not been previously reported to be associated with colorectal cancer. Among these proteins, five were not reported in any type of malignancy. IEF/western blotting confirmed the differences in protein expression between the normal and the tumor tissues. These results may provide an insight for biomarker development and drug target discovery in colorectal cancer.

* *Corresponding author at:* Division of Pharmacoproteomics, National Cancer Center Research Institute, 5-1-1 Tsukiji, Chuo-ku, Tokyo 104-0045, Japan. Tel.: +81 3 3542 2511x3004; fax: +81 3 3547 5298.
E-mail address: takondo@ncc.go.jp (T. Kondo).
[1] Present address: Department of Life Science, Rikkyo St Paul's University, Japan.

1874-3919/$ – see front matter © 2011 Elsevier B.V. All rights reserved.
doi:10.1016/j.jprot.2011.02.030

1. Introduction

Colorectal cancer is the third most common type of cancer and the fourth most frequent cause of cancer death worldwide [1]. Annually, more than one million people are diagnosed with colorectal cancer and approximately half of them die from malignancy [1]. Although intensive treatments including surgery, chemotherapy, and molecular targeting therapy have been developed, outcome remains dismal, particularly for those with distant organ metastasis [2]. Moreover, tumors with similar histological characteristics often show different outcomes and responsiveness to therapy. Therefore, it has long been desired to establish individualized therapy for colorectal cancer [3,4]. The five-year survival for patients with localized disease who had undergone curative surgery can reach 90%, but it is 65% for those with lymph node metastases. This emphasizes the importance of early diagnosis. However, there are no specific symptoms at the early stage of colorectal cancer, and the existing modalities for early diagnosis (e.g., fecal occult blood test and plasma biomarkers) have limited sensitivity and specificity. Characterization of tumor cells with an aim of application of clinical utilities needs to be further challenged for drug target discovery and biomarker development.

With this background, a proteomic approach was applied to colorectal cancer using various modern or refined technologies [5–7]. A proteome is a functional translation of a genome, directly regulating cancer phenotypes. Thus, proteomics may give us insights into the carcinogenesis and progression of colorectal cancer. Various technologies, including gel-based separation methods [8,9], MS [10–12], and array-based methods [13–16] have been applied for global protein expression studies, resulting in the identification of aberrantly regulated proteins. The studies on such protein characteristics may increase our understanding of the molecular basis of colorectal cancer and contribute to better management, and therefore, an improved outcome.

The goal of the present study was to provide the "proteomics community" the profile of proteome expression for colorectal cancer. We reported the proteomic differences between surgically resected normal and tumor tissues from 53 patients with colorectal cancer. For quantitative expression profiling, we employed 2D-DIGE and MS. By focusing on evaluating proteins with alkaline pI, we found six proteins whose aberrant expression had not been reported in colorectal cancer. Although antibody-based validation is critical for protein identification and further clinical examination, discordance between the results of 2D-DIGE and SDS-PAGE/western blotting was often observed. We clarified the backgrounds of such discordance using IEF/western blotting by demonstrating the presence of multiple protein isoforms with different isoelectric points.

2. Materials and methods

2.1. Clinical samples

This study involved 53 patients with colorectal cancer who underwent curative surgery at the National Cancer Center Hospital. The clinicopathological data of the cases is summarized in Table 1, and the data of individual patients are listed in Supplemental Table 1.

Tumor tissues and matched normal mucosal tissues were obtained from 53 cases; 106 samples were examined in this study. The specimens were snap-frozen in liquid nitrogen and stored at −80 °C until use. Clinical staging was determined based on diagnostic imaging criteria: the TMN system. None of the patients received antineoplastic therapy before surgery. This study was approved by the ethics committee of the National Cancer Center.

2.2. Protein extraction

Proteins were extracted from surgically resected tissues as described in a previous study [17]. In brief, the frozen tissues were powdered in liquid nitrogen using Multi-beads Shocker (Yasui-kikai, Osaka, Japan). Tissues were then treated with urea lysis buffer (2 M thiourea, 7 M urea, 3% CHAPS, and 1% Triton X-100). After centrifugation, the supernatant was recovered as a soluble protein fraction and stored at −80 °C until use.

2.3. 2D-DIGE

A protein expression profile was created as described in a previous study [16]. In brief, an internal control sample was created by mixing an equal amount of a small portion of individual samples. Fifteen micrograms of the individual and the internal control samples was labeled with Cy3 and Cy5 fluorescent dyes (CyDye DIGE Fluor saturation dye, GE Healthcare, Uppsala, Sweden), respectively, according to manufacturer's instruction. The differently labeled protein samples were mixed together, divided into three portions, and separated using 2D gel electrophoresis. First-dimension separation was achieved by the IPG dry strip gel, with a pI range of 6–9, and Multiphor II (GE Healthcare). Protein samples were applied to the IPG gels by a cup-loading method at the acidic end, and 50,250 Vh was applied to the IPG gels for IEF. The second-dimension separation was done by SDS-PAGE overnight using the original large format gel apparatus [16], with a

Table 1 – Summary of clinicopathological data of the patients.

Age	
Median	61.4
Gender	
Male	37
Female	16
Site	
Colon	29
Rectum	24
Histological grade	
Well differentiated	40
Moderately	10
Poorly	3
TNM stage	
I	7
II	27
III	17
IV	2

separation distance of 33 cm and a circulating water cooling system.

Following gel electrophoresis, gels sandwiched by low-fluorescence glass plates were scanned using a laser scanner (Typhoon Trio, GE Healthcare), and Cy3 and Cy5 images were obtained by single scans. Cy5 spot intensity was normalized with Cy3 (one for all protein spots) using image analysis software (Progenesis SameSpot, Nonlinear Dynamics, Newcastle, UK). The protein expression profile was exported in the format of an XML file, and imported to data-mining software (Expressionist, GeneData, Basel, Switzerland) for statistical studies. For preparative purposes, 100 μg of protein sample was labeled by Cy3 fluorescent dye, and separated as described above. Protein spots of interest were matched between the images of analytical and preparative gels, and recovered into 96-well plates from the preparative gels using our original spot-recovery machine (Molecular Hunter, As One Corporation, Osaka, Japan) [16]. The recovered protein spots were stored at 4 °C until use.

2.4. *Statistical analysis*

Statistical analyses involved scatter plots, hierarchical clustering, principal component analyses, correlation studies and volcano plots. The Wilcoxon test was carried out by Expressionist software. The Wilcoxon test was used to identify the

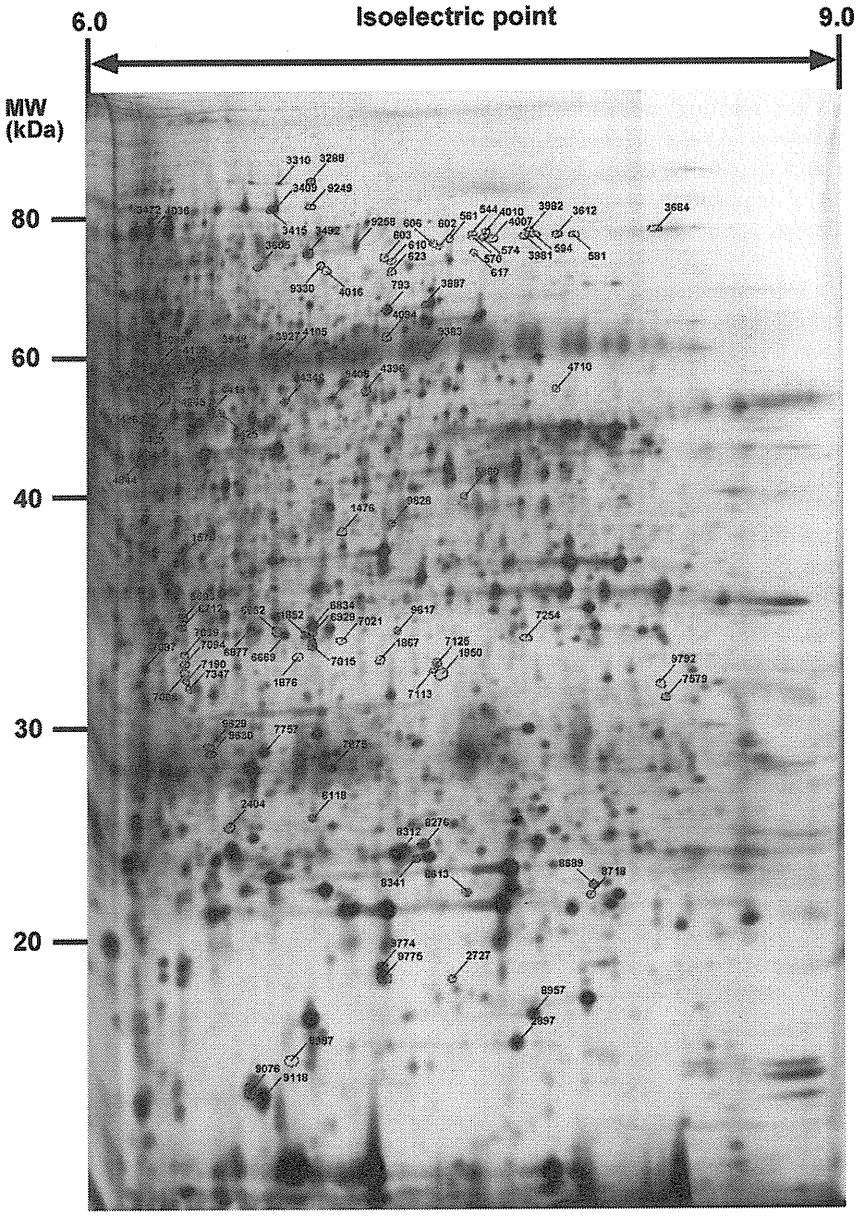

Fig. 1 – 2D image of the Cy3-labled internal control sample was shown. The fluorescently labeled protein sample was separated according to the pI (separation distance of 24 cm) and molecular weight (separation distance of 33 cm). The circled protein spots were later identified differential intensities between normal and tumor tissues. The spot numbers corresponded to those in other figures and tables.

spot intensity which was statistically different between the sample groups.

2.5. *Protein identification using MS*

Proteins were extracted from the protein spots by in-gel digestion as previously reported [16]. In brief, the recovered protein spots were washed extensively with acetonitrile and ammonium bicarbonate minimum solution, and treated with trypsin (Promega, Madison, WI) at 37 °C overnight. Tryptic digests were recovered from the gel pieces, concentrated by a vacuum and re-solubilized with 0.1% trifluoroacetic acid. The final tryptic digests were subjected to LC composed of Paradigm MS4 dual solvent delivery system (Michrom BioResources, Auburn, CA) and an LTQ linear ion trap MS (Thermo Electron, San Jose, CA) equipped with a nano-electrospray ion source (AMR, Tokyo, Japan). Mascot software (version 2.3.0, Matrix Science, London, UK) was used to search for the mass of the peptide ion peaks against the SWISS-PROT database (*Homo sapiens*, 471,472 sequences in Sprot_57.5 fasta file). Search parameters were as follows: trypsin digestion allowing up to three tryptic-mass cleavages, fixed modifications of carbamidomethyl, variable modifications of oxidation, +2 and +3 peptide charge, peptide mass tolerance of 0.8 Da and MS/MS tolerance of 0.8 Da was used for all the tryptic-mass searches.

2.6. *Western blotting*

Protein samples (sample no.; 3N and 3T) extracted using urea lysis buffer were used for western blotting. In brief, protein samples were separated by SDS-PAGE gels with Criterion TGX Precast Gels (Bio-Rad, Hercules, CA) or IPG gels (length, 24 cm; pI range 3–10; GE Healthcare). Five and 50 μg proteins were separated using SDS-PAGE and IEF, respectively. The proteins separated using SDS-PAGE were electrophoretically transferred to a nitrocellulose membrane. The proteins separated using the IPG gels were transferred by diffusion as described in a previous report, with some modifications [17,18]; the transfer was performed using conventional western blotting with a buffer system consisting of 20 mM Tris (pH 7.5), 500 mM sodium chloride, and 20% methanol. After blocking with skimmed milk for 1 h, the membrane was reacted with a primary antibody overnight. The following antibodies were used at the following dilutions; fumarase (1:200; Abcam, Cambridge, UK), electron transfer flavoprotein alpha (1:500; ProteinTech, Chicago, IL), annexin A2 (1:5000; Becton Dickinson, Franklin Lakes, NJ), moesin (1:5000; Becton Dickinson), lamin A/C (1:150; Millipore, Billerica, MA), lung cancer antigen NY-LU-1 (1:100; Abcam), 60 kDa heat shock protein (1:5000; Becton Dickinson), and pyruvate kinase isozymes M1/M2 (1:100; Abcam). The membrane was then treated with the second antibody: rabbit IgG (1:1000; GE Healthcare) and mouse IgG (1:1000; GE Healthcare). The immunocomplexes were detected by enhanced chemiluminescence (ECL Plus; GE Healthcare) and LAS-3000 (FujiFilm, Tokyo, Japan). The intensity of protein bands was measured by ImageQuant software (GE Healthcare). The intensity of individual protein bands in the SDS-PAGE/western blotting was normalized with the intensity of the actin band in identical membranes. Normalization was done using the same amount of loaded proteins in the IPG/western blotting.

3. Results and discussion

Proteomic studies on colorectal cancer using surgically resected tissues have been achieved for biomarker development and drug target discovery. The proteomics of colorectal cancer in this report were characterized by two factors. First, the present study included a large sample size (106 samples) of surgically resected colorectal cancer tissues. We ran triplicate gels amounting to a total of 318 large format gels being examined. Use of 2D-DIGE helped to avoid a labor intensive experiment. In 2D-DIGE, simple laser scanning generates the gel images in less than 1 h for Cy3- and Cy5-labeled protein samples, omitting the rate-limiting step of gel-based proteomics such as gel staining with silver or CBB. In addition, compared to MS, the cost of electrophoresis equipment is relatively low, also the parallel use of multiple devices enabled high-throughput experiments. The second factor in the present study was that we focused on proteins with alkaline pI. By concentrating specifically on the proteomic analyses, we aimed to obtain a unique data that was available from the experiments using IPG gels with a wider range of pI.

A typical 2D-DIGE image of the Cy3-labeled internal control sample is shown in Fig. 1. We observed 1687 protein spots in the alkaline area. System reproducibility was examined by running an identical sample thrice. The scattergram in Fig. 2 demonstrates that the intensity of ≥96% protein spots is scattered within 2-fold differences, and >90.5% within 1.5-fold differences. Similar system reproducibility was observed in our previous proteomic studies, in which a large-format electrophoresis apparatus and internal control sample were used for protein expression profiling [19–22]. A long separation distance of a large-format gel could result in clear focusing of the spots and the internal control sample, which could normalize all protein spots in the present study. This compensated for gel-to-gel variation and resulted in high reproducibility of 2D images. A wide dynamic range of fluorescent signal also contributed to the high reproducibility.

To capture the overall feature of proteome data, we examined unsupervised classification on the basis of the intensity of all 1687 protein spots observed in the present study. The normalized intensity of 1687 protein spots across all gels is available in Supplemental Table 2. Hierarchical clustering grouped the protein samples into "normal" and "tumor tissue" groups (Fig. 3A). Principal component analysis using the intensity of protein spots also divided the samples into normal and tumor tissue groups (Fig. 3B). Visual inspection of the data by hierarchical clustering and principal component analysis suggested that the proteome of normal tissue may be more homogeneous than that of tumor tissues. This may reflect the similar genomic contents of these tissues. These speculations were supported by the data from the correlation matrix, in which the correlation coefficient of spot intensity was calculated for all paired samples and demonstrated by colors (Fig. 3C). Compared with the tumor samples, the proteome contents of normal tissues were more similar to

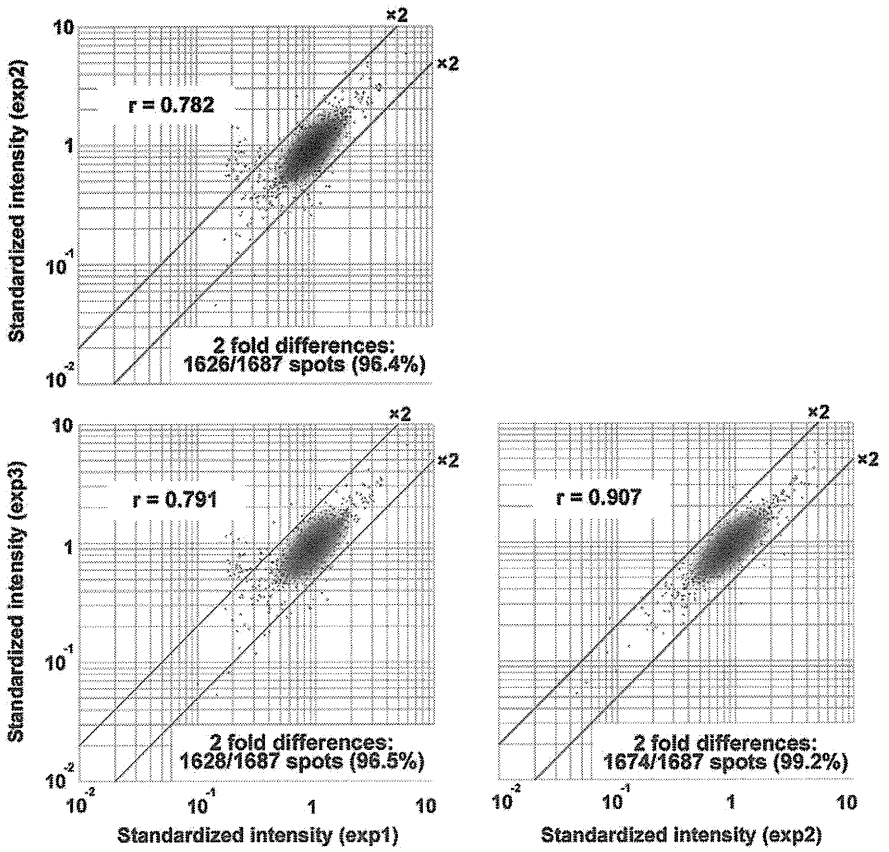

Fig. 2 – System reproducibility was measured by scatter plot. The identical protein sample was independently examined three times, and the spot intensity was compared among the experiments. The correlation coefficient values for the independent experiments were at least 0.78, and at least 96.4% of protein spots intensity was scattered within 2-fold differences.

each other. These observations suggest that the overall proteome features possibly undergoes a drastic change during carcinogenesis.

To identify the protein spots whose intensity was responsible for the results of unsupervised classification (Fig. 3), we compared the normal and the tumor tissue groups. Among 1687 protein spots observed, we detected 100 with statistically ($p<0.01$) and significantly (>2-fold average intensity) different intensities between the normal and the tumor tissue groups (Fig. 4A). We observed 45 and 55 protein spots with higher (Group A in Fig. 4A) and lower intensities (Group B in Fig. 4A) in tumor tissues compared with their normal counterparts, respectively. Except for spots 3981 and 610, the intensity of the 100 protein spots was scattered within 2-fold differences when the identical samples were examined three times (Fig. 2). These 100 protein spots were subjected to protein identification using MS. The row data are available as Supplemental Data. Consequently, 58 unique proteins were identified (right side in Fig. 4A; Table 2 and Supplemental Table 3). These 100 protein spots included five spots with statistically ($p<0.01$) and significantly (>2-fold average intensity) different intensities among stage-II and stage-III patients. The identified proteins were classified according to their association with different types of malignancies. Five proteins had not been previously reported in malignancies, including colorectal cancer (Group D), and one protein was previously reported in another malignancy excluding colorectal cancer (Group C) (Table 2). The observed *pI* was close to the theoretical ones (Table 2), and the use of IPG gels with an alkaline range allowed identification of aberrant regulation of the proteins involved in colorectal cancer.

The results of functional classification of the identified 58 proteins are summarized in Table 2. Limited portions of the proteome were observed by 2D-DIGE and their functional classifications were affected by the characteristics of 2D-DIGE. Hence, we did not make any conclusions on the basis of the

Fig. 3 – Overall features of colorectal cancer proteome visualized by 2D-DIGE were examined by hierarchical clustering (A) and principal component analyses (B). The samples were grouped based on differential intensities of 1687 protein spots. These two analyses demonstrated that the samples were grouped according to the histological classification. C. The correlation matrix demonstrated the similarity of samples along histological classification. D. The volcano plot demonstrated the protein spots with p value and ratio of means between normal and tumor tissues. We selected protein spots with >2-fold intensity difference between the normal and the tumor tissue for further examination.

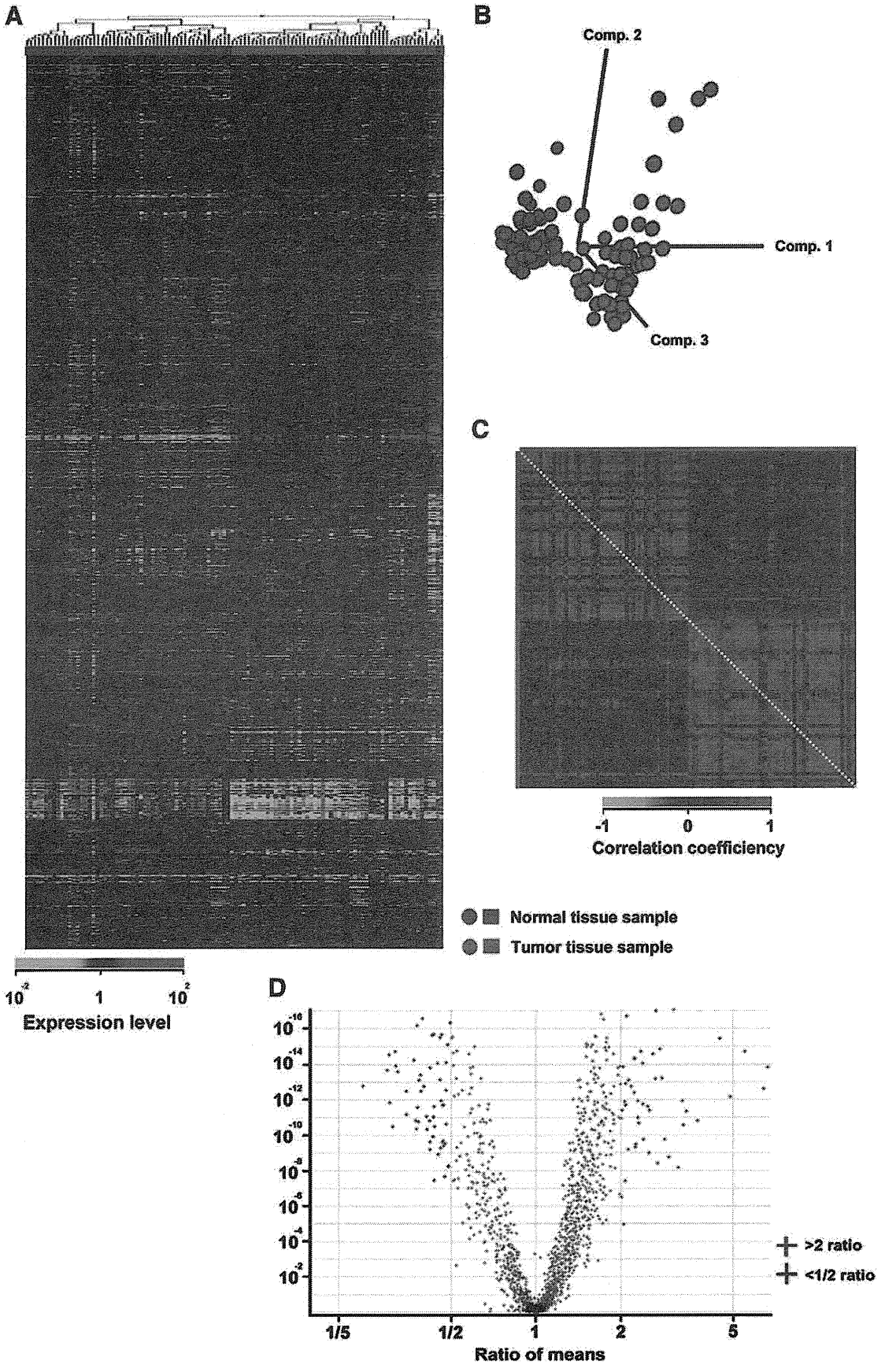

functional classifications regarding the likelihood of certain proteins being involved in colorectal cancer. Proteins with low abundance such as transcription factors, receptors, and the proteins in signal transduction pathways are known to contribute to carcinogenesis and cancer development. However, in our study we did not detect these proteins; this may indicate the limitation of 2D-DIGE. 2D-DIGE permits quantitative observation of multiple protein species and this advantage is unique to 2D-PAGE-based methods. We observed that 19 proteins appeared in multiple protein spots. These multiple proteins may correspond to post-translational modifications that are associated with the molecular mechanisms of malignant phenotypes. Thus, 2D-DIGE remains indispensable for cancer proteomics. The combined use of 2D-DIGE and other methods that counterbalance the limitations of 2D-DIGE should be considered for analyses of cancer proteomics. For instance, we may consider using antibody-based proteomics [23] and multiple reaction monitoring systems [24] to measure the expression level of faint proteins.

To validate the aberrant expression level of identified proteins in tumor tissues, we examined their expression by western blotting. Certain proteins may present as multiple forms with unexpected p*I*, and the intensity of single protein spots may not represent its total expression level. For such proteins, the data of SDS-PAGE/western blotting did not match those of 2D-DIGE (data not shown). This can be avoided by using western blotting and 2D-PAGE gel; however, carrying out western blotting using a large-format 2D gel is challenging because of the fragility of the gel. To compensate for these problems, we employed IPG/western blotting. We separated the proteins according to their p*I* using IPG gels, then transferred those to a membrane and allowed to react with specific antibodies (Fig. 5). Comparison of the intensity in 2D-DIGE and IPG/western blotting demonstrated that among 12 protein spots examined, 11 showed a consistent increase or decrease in intensity between the normal and the tumor tissues. These observations suggest that IPG/western blotting can be used for validation of 2D-DIGE results using antibodies. Only 1 spot, 9383, showed inconsistency between IPG/western blotting and 2D-DIGE results. The experimental factors of western blotting (e.g., transfer efficiency and antibody reactivity) may be the reason for such inconsistencies. To establish the clinical utilities of proteins identified by 2D-DIGE, more number of clinical cases should be used for the purpose of validation. In this report, we examined one protein sample for 12 protein spots to demonstrate the novel application of IPG, and the IPG/western blotting may be useful for such studies. IPG/western blotting can be used for the studies on multiple samples, because the parallel electrophoresis for the IPG can be achieved by a conventional device for isoelectric focusing electrophoresis, such as Multiphor II and Ettan IPGphor III (GE).

For the proteins with p*I* range of 6–9, in addition to the protein bands corresponding to the identified protein spots, we observed bands that were different between normal and tumor tissues (e.g., protein band in Fig. 5, panel e). 2D-DIGE uncovered the proteins with a molecular weight approximately between 10 kDa and 200 kDa (Fig. 1), and the proteins with excess molecular weight may not be uncovered by 2D-DIGE. For the proteins within less than 6 p*I* range, we observed protein bands with different intensities between the normal and the tumor tissues in four proteins (Fig. 5, panels c, d, e, and g). We had not expected to obtain these results from 2D-DIGE experiments. Thus, IPG/western blotting provided additional data on the identified proteins which were not obtained by conventional 2D-DIGE experiments.

We found that among the 58 identified proteins, aberrant expression of six proteins had not been reported in colorectal cancer tissues until now. These proteins were: torsin-1A-interacting protein 1, moesin, calcium-binding mitochondrial carrier protein Aralar1, sulfotransferase 1B1, EF-hand domain-containing family member B, and protein L-isoasparatyl/D-asparatyl methyltransferase. Among these six proteins, only moesin has been reported in malignancies other than colorectal cancer. Moesin is a cell adhesion protein, and upregulation of its expression has been associated with metastatic risk in node-negative breast cancer [25], pancreatic cancer [26], and oral squamous cell carcinoma [27]. Further investigation on moesin may provide novel insights into common mechanisms underlying carcinogenesis and cancer development.

Colorectal cancer has been extensively studied by the proteomic approach [28]. However, the results reported by various studies have not always been in accordance. For instance, Xuezhi et al. reported the aberrant expression of 11 proteins in tumor tissues using 2D-DIGE with a ReadyStrip, pH 7–10 (BioRad) in seven patients with colorectal cancer [29]. From among these 11 proteins, we identified four proteins (enolase 1, fructose-bisphosphate aldolase A, GAPDH, and transgelin) as the colorectal cancer-associated proteins in the present study. Considering that these proteins have been reported in other proteomic studies, the association of these proteins with colorectal cancer could be reliable. Even if the results seem to be discordant, it does not suggest that the experiments were carried out inappropriately. The different number of samples and statistical criteria for different proteins can affect the results of comparison; the clinical status of donors is another factor. In addition, the method followed in the experiments can also affect the results of comparative studies. Further validation studies using standard methods and larger sample size should be undertaken to obtain conclusive results. IPG/western blotting could be a powerful tool for validation because, as opposed to immunohistochemistry and conventional SDS-PAGE/western blotting,

Fig. 4 – Results of spot comparison and protein identification were demonstrated as a format of heat-map. (A) The protein spots whose intensity showed >2-fold differences with statistical significance ($p < 0.01$) were selected, and the level of spot intensity was shown as a heat-map, and the protein names were also shown in the right side of the color panel. Groups A and B indicated the protein spots with higher and lower intensities in the tumor samples, respectively. Total 100 protein spots were then examined using mass spectrometry, resulted in identification of 58 unique proteins. (B) Among the 100 protein spots, five protein spots had the different intensities between the patients with different clinical stages; stage-II and stage-III. Note that when multiple proteins were identified from single protein spots, the proteins with highest Mascot score are appeared in the figure. The proteins with different Mascot score are summarized in Supplemental Table 3.

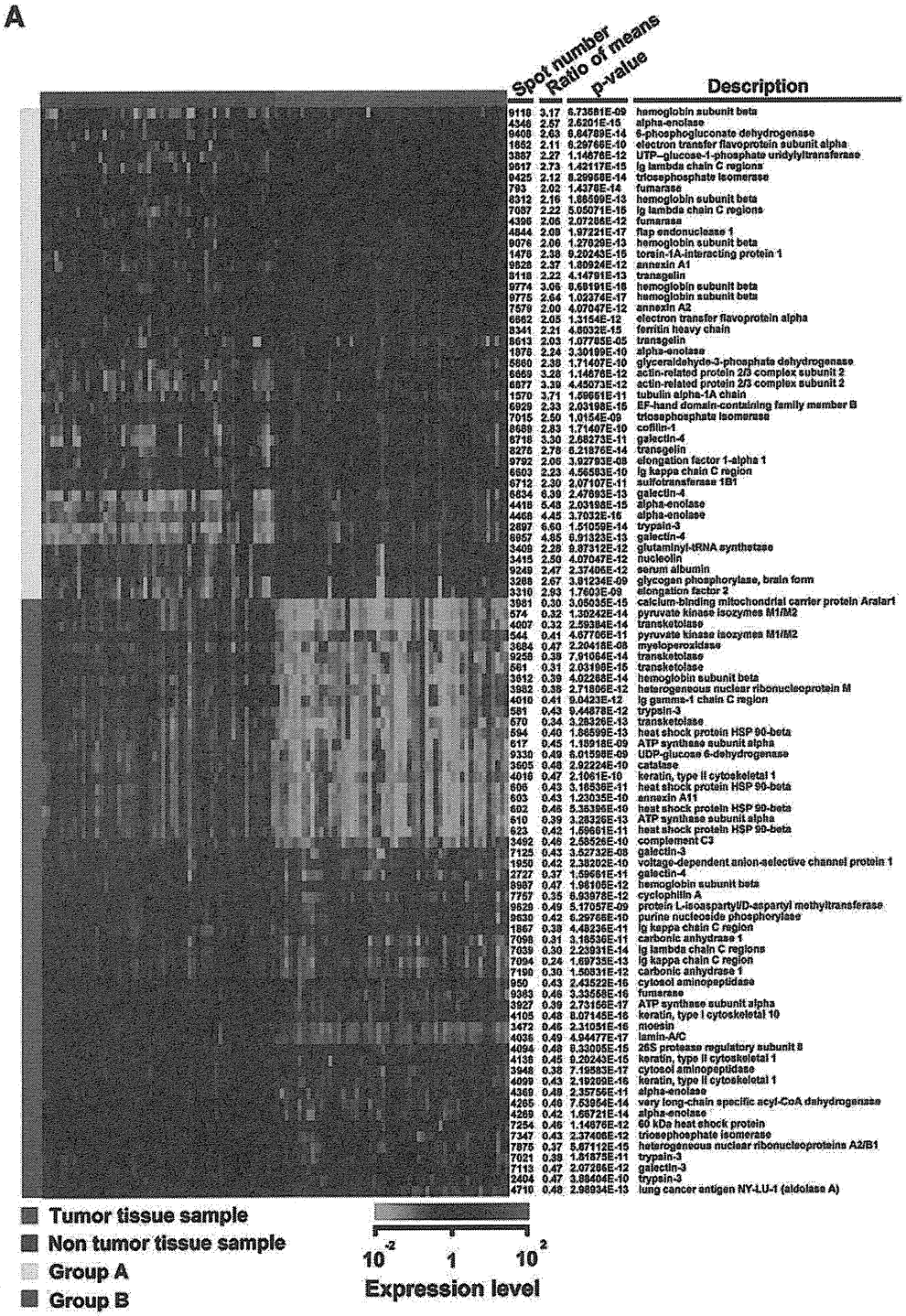

Table 2 – List of proteins from human CRC tissue resolved on pH 6–9 2D-DIGE gels and identified by LTQ linear ion trap mass spectrometer.

Spot no.[a]	Accession no.[b]	Protein description[b]	Protein score[c]	No. of matched peptides	Sequence coverage (%)[d]	MW (Da)[e]	Reference pI[e]	Actual pI[f]	Molecular function[g]	Reports by 2D-PAGE[h]	Reports in CRC[i]
544	P14618	Pyruvate kinase isozymes M1/M2	933	21	32.2	58,470	7.96	7.54	Enzyme	[9,30,32]	A [9,30,32–35]
561	P29401	Transketolase	616	11	24.4	68,519	7.58	7.46	Enzyme	[36,38]	A [34,36–38]
570	P29401	Transketolase	907	18	30.8	68,519	7.58	7.54	Enzyme	[36,38]	A [34,36–38]
574	P14618	Pyruvate kinase isozymes M1/M2	99	2	3.4	58,470	7.96	7.60	Enzyme	[9,30,32]	A [9,30,32–35]
581	P35030	Trypsin-3	119	2	6.6	33,306	7.46	7.95	Metal binding	Not reported	B [39,40]
594	P08238	Heat shock protein HSP 90-beta	1322	23	34.5	83,554	4.97	7.80	ATP binding	[36]	A [34,36]
602	P07900	Heat shock protein HSP 90-alpha	223	3	5.2	83,554	4.97	7.41	ATP binding	[36]	A [34,36,41]
603	P50995	Annexin A11	590	12	19.2	54,697	7.53	7.20	Metal binding	[38,42]	A [38,42,43]
606	P08238	Heat shock protein HSP 90-beta	883	17	24.6	83,554	4.97	7.39	ATP binding	[36]	A [34,36]
610	P25705	ATP synthase subunit alpha	1115	25	40.9	59,828	9.16	7.22	ATP binding	[36,38,44]	A [36,38,44]
617	P25705	ATP synthase subunit alpha	1022	18	36.2	59,828	9.16	7.56	ATP binding	[36,38,44]	A [36,38,44]
623	P08238	Heat shock protein HSP 90-beta	1322	23	34.5	83,554	4.97	7.22	ATP binding	[36]	A [34,36]
793	P07954	Fumarase	316	5	14.3	54,773	8.85	7.20	Enzyme	[36,38]	A [34,36,38, 45–47]
950	P28838	Cytosol aminopeptidase	504	12	20.4	56,530	8.03	6.41	Metal binding	[36]	A [34,36]
1476	Q5JTV8	Torsin-1A-interacting protein 1	106	3	3.9	66,379	8.22	7.01	Other	Not reported	D
1570	Q71U36	Tubulin alpha-1A chain	410	14	24.2	50,788	4.94	6.36	Nucleic acid binding	Not reported	B [34,48–50]
1852	P13804	Electron transfer flavoprotein subunit alpha	256	4	15.6	35,400	8.62	6.86	Electron carrier activity	[38]	A [34,38,51]
1867	P01834	Ig kappa chain C region	122	2	32.1	11,773	5.58	7.16	Antigen binding	[52]	A [30,34,52–54]
1876	P06733	Alpha-enolase	811	21	38.5	47,481	7.01	6.82	Enzyme	[8,29,30,36]	A [8,29,30,36]
1950	P21796	Voltage-dependent anion-selective channel protein 1	637	8	40.6	30,868	8.62	7.41	Other	[11,29,38]	A [11,29,38]
2404	P35030	Trypsin-3	113	2	6.9	33,306	7.46	6.56	Metal binding	Not reported	B [39,40]
2727	P56470	Galectin-4	159	2	11.8	36,032	9.21	7.45	Sugar binding	[38]	A [34,38]
2897	P35030	Trypsin-3	113	2	6.9	33,306	7.46	7.73	Metal binding	Not reported	B [39,40]
3288	P11216	Glycogen phosphorylase, brain form	1297	26	33.8	97,319	6.40	6.90	Enzyme	[38]	A [34,38,55]
3310	P13639	Elongation factor 2	3671	27	25.5	96,246	6.41	6.77	Nucleic acid binding	[8,30,38]	A [8,30,38]
3409	P47897	Glutaminyl-tRNA synthetase	179	4	5.9	88,655	6.71	6.75	ATP binding	[38]	A [38]
3415	P19338	nucleolin	446	9	14.2	76,625	4.60	6.73	Nucleic acid binding	Not reported	B [34]
3472	P26038	Moesin	685	13	24.1	67,892	6.08	6.23	Antigen binding	Not reported	C [56–59]
3492	P01024	Complement C3	211	4	2.6	188,569	6.02	6.88	Antigen binding	[29]	A [29,34,53,60,61]
3605	P04040	Catalase	485	9	18.0	59,947	6.90	6.68	Enzyme	[36,38]	A [30,36,38,46,62]
3612	P68871	Hemoglobin subunit beta	215	4	28.6	16,102	6.75	7.88	Metal binding	[30,36,52]	A [30,36,52]
3684	P05164	Myeloperoxidase	213	4	5.8	84,784	9.19	8.27	Enzyme	Not reported	B [63]
3887	Q16851	UTP–glucose-1-phosphate uridylyltransferase	343	6	13.8	57,076	8.16	7.35	Enzyme	[38]	A [38]
3927	P25705	ATP synthase subunit alpha	428	6	12.8	59,828	9.16	6.73	ATP binding	[36,38,44]	A [36,38,44]
3948	P28838	Cytosol aminopeptidase	448	8	21.0	56,530	8.03	6.51	Metal binding	[36]	A [34,36]

3981	O75746	Calcium-binding mitochondrial carrier protein Aralar1	276	5	8.0	75,144	8.58	7.76	Metal binding	Not reported	D
3982	P52272	Heterogeneous nuclear ribonucleoprotein M	82	2	4.1	77,749	8.84	7.78	Nucleic acid binding	Not reported	B [34]
4007	P29401	Transketolase	317	5	12.4	68,519	7.58	7.63	Enzyme	[36,38]	A [34,36–38]
4010	P01857	Ig gamma-1 chain C region	182	5	17.6	36,596	8.46	7.59	Antigen binding	Not reported	B [34,49,53]
4016	P04264	Keratin, type II cytoskeletal 1	220	4	6.2	66,170	8.15	6.96	Sugar binding	[52]	A [34,52]
4036	P02545	Lamin A/C	375	8	17.5	74,380	6.57	6.24	other	[38]	A [34,38,64]
4094	P62195	26S protease regulatory subunit 8	974	19	47.8	45,768	7.11	7.20	ATP binding	[36]	A [36]
4099	P04264	Keratin, type II cytoskeletal 1	92	2	3.4	66,170	8.15	6.28	Sugar binding	[52]	A [34,52]
4105	P13645	Keratin, type I cytoskeletal 10	123	3	3.4	59,046	5.09	6.81	Sugar binding	[52]	A [34,52]
4136	P04264	Keratin, type II cytoskeletal 1	120	2	4.0	66,170	8.15	6.32	Sugar binding	[52]	A [34,52]
4265	P49748	Very long-chain specific acyl-CoA dehydrogenase	810	15	25.6	70,745	8.92	6.30	Enzyme	[38]	A [38,65]
4269	P06733	Alpha-enolase	530	10	24.2	47,481	7.01	6.28	Enzyme	[8,29,30,36]	A [8,29,30,36]
4346	P06733	Alpha-enolase	525	8	21.2	47,481	7.01	6.79	Enzyme	[8,29,30,36]	A [8,29,30,36]
4369	P06733	Alpha-enolase	850	16	36.9	47,481	7.01	6.30	Enzyme	[8,29,30,36]	A [8,29,30,36]
4396	P07954	Fumarase	290	5	17.8	54,773	8.85	7.11	Enzyme	[36,38]	A [34,36,38, 45–47]
4418	P06733	Alpha-enolase	222	3	10.6	47,481	7.01	6.49	Enzyme	[8,29,30,36]	A [8,29,30,36]
4468	P06733	Alpha-enolase	621	15	26.0	47,481	7.01	6.36	Enzyme	[8,29,30,36]	A [8,29,30,36]
4710	P04075	Lung cancer antigen NY-LU-1 (aldolase A)	229	4	15.4	39,851	8.30	7.88	Enzyme	[29,30,38]	A [29,30,38]
4844	P39748	Flap endonuclease 1	108	2	5.8	42,908	8.80	6.23	Nucleic acid binding	Not reported	B [66,67]
5860	P04406	Glyceraldehyde-3-phosphate dehydrogenase	400	6	31.3	36,201	8.57	7.50	Enzyme	[29,30,52,68]	A [29,30,41,52,68]
6603	P01834	Ig kappa chain C region	122	2	32.1	11,773	5.58	6.38	Antigen binding	[52]	A [30,34,52–54]
6662	P13804	Electron transfer flavoprotein subunit alpha	108	2	7.5	35,400	8.62	6.75	Electron carrier activity	[38]	A [34,38,51]
6669	O15144	Actin-related protein 2/3 complex subunit 2	114	3	10.3	34,426	6.84	6.79	Actin binding	[36]	A [36,69,70]
6712	O43704	Sulfotransferase 1B1	141	3	13.2	35,048	6.57	6.38	Enzyme	Not reported	D
6834	P56470	Galectin-4	171	2	11.8	36,032	9.21	6.90	Sugar binding	[38]	A [34,38]
6877	O15144	Actin-related protein 2/3 complex subunit 2	279	7	20.0	34,426	6.84	6.66	Actin binding	[36]	A [36,69,70]
6929	Q8N7U6	EF-hand domain-containing family member B	66	2	1.8	94,558	7.50	6.90	Metal binding	Not reported	D
7015	P60174	Triosephosphate isomerase	443	9	32.9	26,938	6.45	6.90	Enzyme	[29,30,35,71,72]	A [29,30,34,68, 71–73]
7021	P35030	Trypsin-3	128	2	6.6	33,306	7.46	7.01	Metal binding	Not reported	B [39,40]
7039	P0CG04	Ig lambda chain C regions	142	2	23.8	11,401	6.92	6.40	Antigen binding	Not reported	B [34,53,54]
7087	P0CG04	Ig lambda chain C regions	226	3	41.9	11,401	6.92	6.23	Antigen binding	Not reported	B [34,53,54]
7094	P01834	Ig kappa chain C region	169	3	32.1	11,773	5.58	6.40	Antigen binding	[52]	A [30,34,52–54]
7098	P00915	Carbonic anhydrase 1	272	5	25.7	28,909	6.59	6.40	Enzyme	[32,38,74]	A [32,38,74–77]
7113	P17931	Galectin-3	166	4	16.0	26,193	8.57	7.37	Sugar binding	[29,38,78]	A [29,34,38,78]
7125	P17931	Galectin-3	166	4	14.8	26,193	8.57	7.39	Sugar binding	[29,38,78]	A [29,34,38,78]
7190	P00915	Carbonic anhydrase 1	282	5	26.1	28,909	6.59	6.40	Enzyme	[32,38,74]	A [32,38,74–77]
7254	P10809	60 kDa heat shock protein	493	9	17.8	61,187	5.70	7.74	ATP binding	[29,52,72,79]	A [29,52,72,79, 80]

(continued on next page)

Table 2 (*continued*)

Spot no.[a]	Accession no.[b]	Protein description[b]	Protein score[c]	No. of matched peptides	Sequence coverage (%)[d]	MW (Da)[e]	Reference pI[e]	Actual pI[f]	Molecular function[g]	Reports by 2D-PAGE[h]	Reports in CRC[i]
7347	P60174	Triosephosphate isomerase	200	3	22.5	26,938	6.45	6.41	Enzyme	[29,30,35,71,72]	A [29,30,34,68, 71–73]
7579	P07355	Annexin A2	112	2	6.2	38,808	7.57	8.31	Metal binding	[8,9,29,42,74]	A [8,9,29,42,74]
7757	P62937	Cyclophilin A	215	4	28.5	18,229	7.68	6.70	Enzyme	[34,81]	A [31,34,36,81,82]
7875	P22626	Heterogeneous nuclear ribonucleoproteins A2/B1	117	2	8.8	37,464	8.97	6.98	Nucleic acid binding	[29,38]	A [29,38,83–85]
8118	Q01995	Transgelin	94	2	9.5	22,653	8.87	6.90	Actin binding	[29,30,32,86,88]	A [29,30,32,34, 86–88]
8276	Q01995	Transgelin	117	2	9.5	22,653	8.87	7.33	Actin binding	[29,30,32,86,88]	A [29,30,32,34, 86–88]
8312	P68871	Hemoglobin subunit beta	205	4	31.3	16,102	6.75	7.24	Metal binding	[30,36,52]	A [30,36,52]
8341	P02794	Ferritin heavy chain	158	3	21.3	21,883	5.30	7.31	Enzyme	[9,36]	A [9,34,36,38]
8613	Q01995	Transgelin	84	2	8.5	22,653	8.87	7.50	Actin binding	[29,30,32,86,88]	A [29,30,32,34, 86–88]
8689	P23528	Cofilin-1	155	3	25.3	18,719	8.22	8.02	Actin binding	[29,38,52,71]	A [29,34,38,52,71]
8718	P56470	Galectin-4	124	5	19.2	36,032	9.21	8.01	Sugar binding	[38]	A [34,38]
8957	P56470	Galectin-4	110	2	7.4	36,032	9.21	7.78	Sugar binding	[38]	A [34,38]
8987	P68871	Hemoglobin subunit beta	349	6	53.1	16,102	6.75	6.81	Metal binding	[30,36,52]	A [30,36,52]
9076	P68871	Hemoglobin subunit beta	320	5	48.3	16,102	6.75	6.64	Metal binding	[30,36,52]	A [30,36,52]
9118	P68871	Hemoglobin subunit beta	170	3	28.6	16,102	6.75	6.70	Metal binding	[30,36,52]	A [30,36,52]
9249	P02768	Serum albumin	643	13	19.2	71,317	5.92	6.90	Nucleic acid binding	[9]	A [9,51,90]
9258	P29401	Transketolase	341	6	16.4	68,519	7.58	7.07	Enzyme	[36,38]	A [34,36–38]

9330	O60701	UDP-glucose 6-dehydrogenase	515	9	27.7	55,674	6.73	6.94	Enzyme	[29,38]	A [29,34,38,89]
9383	P07954	Fumarase	509	8	24.7	54,773	8.85	7.37	Enzyme	[36,38]	A [34,36,38, 45–47]
9408	P52209	6-Phosphogluconate dehydrogenase	336	4	15.3	53,619	6.80	6.98	Enzyme	Not reported	B [34]
9425	P60174	Triosephosphate isomerase	228	4	15.7	26,938	6.45	6.53	Enzyme	[29,30,35,71,72]	A [29,30,34,68, 71–73]
9617	P0CG04	Ig lambda chain C regions	127	2	23.8	11,401	6.92	7.24	Antigen binding	Not reported	B [34,53,54]
9629	P22061	Protein L-isoaspartyl/D-aspartyl methyltransferase	229	4	22.9	24,806	6.70	6.49	Enzyme	Not reported	D
9630	P00491	Purine nucleoside phosphorylase	485	11	42.9	32,325	6.45	6.49	Nucleic acid binding	[36]	A [36]
9774	P68871	Hemoglobin subunit beta	133	2	19.7	16,102	6.75	7.18	Metal binding	[30,36,52]	A [30,36,52]
9775	P68871	Hemoglobin subunit beta	154	2	17.0	16,102	6.75	7.18	Metal binding	[30,36,52]	A [30,36,52]
9792	P68104	Elongation factor 1-alpha 1	180	3	8.4	50,451	9.10	8.29	Nucleic acid binding	[36,38]	A [31,34,36]
9828	P04083	Annexin A1	304	5	20.2	38,918	6.57	7.22	Metal binding	[36,42,49,78]	A [36,42,49,78]

[a] Spot numbers were referred to those in Figs. 1 and 3.
[b] Accession numbers of proteins and protein name were derived from Swiss-Prot.
[c] Protein score for the identified proteins was based on the peptide ions score ($P<0.05$) (http://www.matrixscience.com).
[d] Reference isoelectric point and molecular weight were obtained from Swiss-Prot.
[e] Sequence coverage was derived from amino acids sequence.
[f] Actual isoelectric point was calculated from 2D-DIGE gel scanning image.
[g] Molecular function was categorized by accessing Gene Ontology database (http://www.geneontology.org/) and literature curation.
[h] Proteins previously reported in 2D-PAGE based proteomics study using CRC tissue.
[i] Proteins previously reported in 2D-PAGE based proteomics study using CRC only (A), those in CRC (B), those in other cancer only (C), and the proteins previously not reported the correlation with cancer (D).

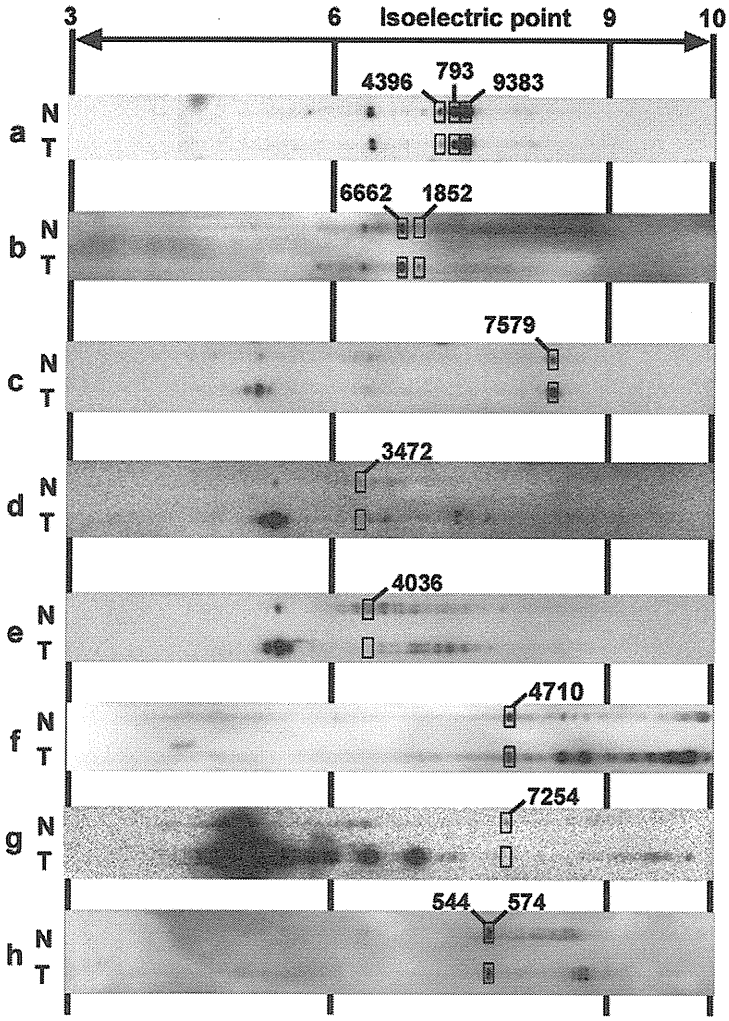

Spot number	T/N ratio IPG WB	T/N ratio 2D-DIGE
793	1.71	3.00
4396	4.27	1.65
9383	2.90	0.27
1852	5.92	1.99
6662	2.13	2.00
7579	2.51	1.56
3472	0.49	0.73
4036	0.17	0.61
4710	0.12	0.60
7254	0.42	0.27
544	0.68	0.28
574	0.68	0.20

Fig. 5 – The validation study was performed using specific antibodies after the proteins separated according to their pI. Ratios of intensity between normal (N) and tumor tissue (T) samples are shown in the left side for all protein bands (IPG/WB) and spots (2D-DIGE) as T/N ratio. Spot number corresponded to those in other figures and tables. Covered pI range of the present study is between 6 and 9, and the corresponding area is indicated in the figure. Protein names are as follows; a. fumarase, b. electron transfer flavoprotein subunit alpha, c. annexin A2, d. moesin, e. lamin A/C, f. lung cancer antigen NY-LU-1, g. 60 kDa heat shock protein, and h. pyruvate kinase isozymes M1/M2. Note that the protein intensity in the IPG/western blotting and the 2D-DIGE was quite concordant except spot, 9383. Sample numbers 3N and 3T are used for these analyses.

it reproduces 2D-PAGE results by separating proteins according to their pI.

4. Conclusions

We reported the proteomic differences of normal and tumor tissues of patients with colorectal cancer. Focusing specifically on proteins with alkaline pI and using 2D-DIGE with a large-format electrophoresis apparatus in a relatively large sample size, we observed novel aberrant regulation of six proteins in colorectal cancer tissues. Further investigation of these proteins may provide more insights in colorectal cancer, and contribute to development of biomarkers and drug target discovery. We also demonstrated the utility of IPG/western blotting for cancer proteomics. IPG/western blotting may be a useful tool to confirm the 2D-DIGE results, since it permits measurement of the amount of individual protein species, and enables study of the proteins which cannot be identified by 2D-DIGE.

Supplementary materials related to this article can be found online at doi: 10.1016/j.jprot.2011.02.030.

Acknowledgments

This study was supported by a grant from the Program for the Promotion of Fundamental Studies in Health Sciences conducted by the National Institute of Biomedical Innovation of Japan, as well as a grant from the Third-term Comprehensive 10-Year Strategy for Cancer Control from the Ministry of Health, Labor, and Welfare of Japan.

REFERENCES

[1] Weitz J, Koch M, Debus J, Hohler T, Galle PR, Buchler MW. Colorectal cancer. Lancet 2005;365:153–65.
[2] Pfister DG, Benson III AB, Somerfield MR. Clinical practice. Surveillance strategies after curative treatment of colorectal cancer. N Engl J Med 2004;350:2375–82.
[3] Liefers GJ, Tollenaar RA. Cancer genetics and their application to individualised medicine. Eur J Cancer 2002;38:872–9.
[4] Popa-Velea O, Cernat B, Tambu A. Influence of personalized therapeutic approach on quality of life and psychiatric comorbidity in patients with advanced colonic cancer requiring palliative care. J Med Life 2010;3:343–7.
[5] Barderas R, Babel I, Casal JI. Colorectal cancer proteomics, molecular characterization and biomarker discovery. Proteomics Clin Appl 2010;4:159–78.
[6] Bitarte N, Bandres E, Zarate R, Ramirez N, Garcia-Foncillas J. Moving forward in colorectal cancer research, what proteomics has to tell. World J Gastroenterol 2007;13:5813–21.
[7] Nibbe RK, Koyuturk M, Chance MR. An integrative -omics approach to identify functional sub-networks in human colorectal cancer. PLoS Comput Biol 2010;6:e1000639.
[8] Alfonso P, Canamero M, Fernandez-Carbonie F, Nunez A, Casal JI. Proteome analysis of membrane fractions in colorectal carcinomas by using 2D-DIGE saturation labeling. J Proteome Res 2008;7:4247–55.
[9] Ma Y, Zhao M, Zhong J, Shi L, Luo Q, Liu J, et al. Proteomic profiling of proteins associated with lymph node metastasis in colorectal cancer. J Cell Biochem 2010;110:1512–9.
[10] Ang CS, Nice EC. Targeted in-gel MRM: a hypothesis driven approach for colorectal cancer biomarker discovery in human feces. J Proteome Res 2010;9:4346–55.
[11] Chen JS, Chen KT, Fan CW, Han CL, Chen YJ, Yu JS, et al. Comparison of membrane fraction proteomic profiles of normal and cancerous human colorectal tissues with gel-assisted digestion and iTRAQ labeling mass spectrometry. FEBS J 2010;277: 3028–38.
[12] Xie LQ, Zhao C, Cai SJ, Xu Y, Huang LY, Bian JS, et al. Novel proteomic strategy reveal combined alpha1 antitrypsin and cathepsin D as biomarkers for colorectal cancer early screening. J Proteome Res 2010;9:4701–9.
[13] Pedersen JW, Blixt O, Bennett EP, Tarp MA, Dar I, Mandel U, et al. Seromic profiling of colorectal cancer patients with novel glycopeptide microarray. Int J Cancer 2011;128:1860–71.
[14] Spisak S, Galamb B, Sipos F, Galamb O, Wichmann B, Solymosi N, et al. Applicability of antibody and mRNA expression microarrays for identifying diagnostic and progression markers of early and late stage colorectal cancer. Dis Markers 2010;28:1–14.
[15] Morishita A, Gong J, Nomura T, Yoshida H, Izuishi K, Suzuki Y, et al. The use of protein array to identify targetable receptor tyrosine kinases for treatment of human colon cancer. Int J Oncol 2010;37:829–35.
[16] Kondo T, Hirohashi S. Application of highly sensitive fluorescent dyes (CyDye DIGE Fluor saturation dyes) to laser microdissection and two-dimensional difference gel electrophoresis (2D-DIGE) for cancer proteomics. Nat Protoc 2007;1:2940–56.
[17] Kinzkofer-Peresch A, Patestos NP, Fauth M, Kogel F, Zok R, Radola BJ. Native protein blotting after isoelectric focusing in fabric reinforced polyacrylamide gels in carrier ampholyte generated or immobilized pH gradients. Electrophoresis 1988;9:497–511.
[18] Cowdrey G, Gould B, Rees J, Firth G. The separation and detection of alkaline oligoclonal IgG bands in cerebrospinal fluid using immobilised pH gradients. Electrophoresis 1990;11:813–8.
[19] Orimo T, Ojima H, Hiraoka N, Saito S, Kosuge T, Kakisaka T, et al. Proteomic profiling reveals the prognostic value of adenomatous polyposis coli-end-binding protein 1 in hepatocellular carcinoma. Hepatology 2008;48:1851–63.
[20] Suehara Y, Kondo T, Seki K, Shibata T, Fujii K, Gotoh M, et al. Pfetin as a prognostic biomarker of gastrointestinal stromal tumors revealed by proteomics. Clin Cancer Res 2008;14: 1707–17.
[21] Yamada M, Fujii K, Koyama K, Hirohashi S, Kondo T. The proteomic profile of pancreatic cancer cell lines corresponding to carcinogenesis and metastasis. J Proteomics Bioinform 2009;02:001–18.
[22] Uemura N, Nakanishi Y, Kato H, Saito S, Nagino M, Hirohashi S, et al. Transglutaminase 3 as a prognostic biomarker in esophageal cancer revealed by proteomics. Int J Cancer 2009;124:2106–15.
[23] Lundberg E, Uhlen M. Creation of an antibody-based subcellular protein atlas. Proteomics 2010;10:3984–96.
[24] Picotti P, Rinner O, Stallmach R, Dautel F, Farrah T, Domon B, et al. High-throughput generation of selected reaction-monitoring assays for proteins and proteomes. Nat Methods 2010;7:43–6.
[25] Charpin C, Secq V, Giusiano S, Carpentier S, Andrac L, Lavaut MN, et al. A signature predictive of disease outcome in breast carcinomas, identified by quantitative immunocytochemical assays. Int J Cancer 2009;124:2124–34.
[26] Cui Y, Wu J, Zong M, Song G, Jia Q, Jiang J, et al. Proteomic profiling in pancreatic cancer with and without lymph node metastasis. Int J Cancer 2009;1:1614–21.
[27] Kobayashi H, Sagara J, Kurita H, Morifuji M, Ohishi M, Kurashina K, et al. Clinical significance of cellular distribution of moesin in patients with oral squamous cell carcinoma. Clin Cancer Res 2004;10:572–80.
[28] Jimenez CR, Knol JC, Meijer GA, Fijneman RJ. Proteomics of colorectal cancer: overview of discovery studies and identification of commonly identified cancer-associated proteins and candidate CRC serum markers. J Proteomics 2010;73:1873–95.
[29] Bi X, Lin Q, Foo TW, Joshi S, You T, Shen HM, et al. Proteomic analysis of colorectal cancer reveals alterations in metabolic pathways: mechanism of tumorigenesis. Mol Cell Proteomics 2006;5:1119–30.
[30] Kim HJ, Kang HJ, Lee H, Lee ST, Yu MH, Kim H, et al. Identification of S100A8 and S100A9 as serological markers for colorectal cancer. J Proteome Res 2009;8:1368–79.
[31] Li M, Zhai Q, Bharadwaj U, Wang H, Li F, Fisher WE, et al. Cyclophilin A is overexpressed in human pancreatic cancer cells and stimulates cell proliferation through CD147. Cancer 2006;106:2284–94.
[32] Kim H, Kang HJ, You KT, Kim SH, Lee KY, Kim TI, et al. Suppression of human selenium-binding protein 1 is a late event in colorectal carcinogenesis and is associated with poor survival. Proteomics 2006;6:3466–76.
[33] Christofk HR, Vander Heiden MG, Harris MH, Ramanathan A, Gerszten RE, Wei R. The M2 splice isoform of pyruvate kinase is important for cancer metabolism and tumour growth. Nature 2008;452:230–4.
[34] Thierolf M, Hagmann ML, Pfeffer M, Berntenis N, Wild N, Roeßler M, et al. Towards a comprehensive proteome of normal and malignant human colon tissue by 2-D-LC–ESI-MS and 2-DE proteomics and identification of S100A12 as potential cancer biomarker. Proteomics Clin Appl 2008;2: 11–22.
[35] Zhao L, Wang H, Sun X, Ding Y. Comparative proteomic analysis identifies proteins associated with the development and progression of colorectal carcinoma. FEBS J 2010;20: 4195–204.
[36] Roessler M, Rollinger W, Palme S, Hagmann ML, Berndt P, Engel AM, et al. Identification of nicotinamide N-methyltransferase as a novel serum tumor marker for colorectal cancer. Clin Cancer Res 2005;11:6550–7.

[37] Langbein S, Zerilli M, Hausen A, Staiger W, Rensch-Boschert K, Lukan N, et al. Expression of transketolase TKTL1 predicts colon and urothelial cancer patient survival: Warburg effect reinterpreted. Br J Cancer 2006;94:578–85.
[38] Li XM, Patel BB, Blagoi EL, Patterson MD, Seeholzer SH, Zhang T, et al. Analyzing alkaline proteins in human colon crypt proteome. J Proteome Res 2004;3:821–33.
[39] Gaber A, Nodin B, Hotakainen K, Nilsson1 E, Stenman UF, Bjartell A, et al. Increased serum levels of tumour-associated trypsin inhibitor independently predict a poor prognosis in colorectal cancer patients. BMC Cancer 2010;10:498.
[40] Soreide K, Janssen EA, Korner H, Baak JPA. Trypsin in colorectal cancer: molecular biological mechanisms of proliferation, invasion, and metastasis. J Pathol 2006;209:147–56.
[41] Hoffmann P, Ji H, Moritz RL, Connolly LM, Frecklington DF, Layton MJ, et al. Continuous free-flow electrophoresis separation of cytosolic proteins from the human colon carcinoma cell line LIM 1215: a non two-dimensional gel electrophoresis-based proteome analysis strategy. Proteomics 2001;1:807–18.
[42] Duncan R, Carpenter B, Main LC, Telfer C, Murray GI. Characterisation and protein expression profiling of annexins in colorectal cancer. Br J Cancer 2008;98:426–33.
[43] Song J, Shih IM, Chan DW, Zhang Z. Suppression of annexin A11 in ovarian cancer: implications in chemoresistance. Neoplasia 2009;11:605–14.
[44] Chang HJ, Lee MR, Hong SH, Yoo BC, Shin YK, Jeong JY, et al. Identification of mitochondrial FoF1-ATP synthase involved in liver metastasis of colorectal cancer. Cancer Sci 2007;98: 1184–91.
[45] Yang Y, Valera VA, Padilla-Nash HM, Sourbier C, Vocke CD, Vira MA, et al. UOK 262 cell line, fumarate hydratase deficient (FH^-/FH^-) hereditary leiomyomatosis renal cell carcinoma: in vitro and in vivo model of an aberrant energy metabolic pathway in human cancer. Cancer Genet Cytogenet 2010;196: 45–55.
[46] Patel BB, Li XM, Dixon MP, Blagoi EL, Seeholzer SH, Chen Y, et al. Searchable high-resolution 2D gel proteome of the human colon crypt. J Proteome Res 2007;6:2232–8.
[47] Pollard PJ, Wortham NC, Tomlinson IP. The TCA cycle and tumorigenesis: the examples of fumarate hydratase and succinate dehydrogenase. Ann Med 2003;35:632–9.
[48] Guirons JS, Zeqiraj E, Schumacher U, Greenwell P, Dwek M. Proteome analysis of metastatic colorectal cancer cells recognized by the lectin Helix pomatia agglutinin (HPA). Proteomics 2007;7:4082–9.
[49] He ZY, Wen H, Shi CB, Wang J. Up-regulation of hnRNP A1, ezrin, tubulin β-2C and annexin A1 in sentinel lymph nodes of colorectal cancer. World Gastoroenterol 2010;16: 4670–6.
[50] Volmer MW, Stuhler K, Zapatka M, Schoneck A, Klein-Scory S, Schmiegel W, et al. Differential proteome analysis of conditioned media to detect Smad4 regulated secreted biomarkers in colon cancer. Proteomics 2005;5:2587–601.
[51] Kim J, Kim SH, Lee SU, Ha1 GH, Kang DG, Ha1 NY, et al. Proteome analysis of human liver tumor tissue by two-dimensional gel electrophoresis and matrixassisted laser desorption/ionization-mass spectrometry for identification of disease-related proteins. Electrophoresis 2002;23:4142–56.
[52] Gourley GR, Yang L, Higgins LA, Riviere MA, David LL. Proteomic analysis of biopsied human colonic mucosa. J Pediatr Gastroenterol Nutr 2010;51:46–54.
[53] Okano T, Kondo T, Kakisaka T, Fujii K, Yamada M, Kato H, et al. Plasma proteomics of lung cancer by a linkage of multi-dimensional liquid chromatography and two-dimensional difference gel electrophoresis. Proteomics 2006;6:3938–48.
[54] Yang SB, Chen X, Wu BY, Wang MW, Cai CH, Cho DB, et al. Immunoglobulin kappa and immunoglobulin lambda are required for expression of the anti-apoptotic molecule Bcl-xL in human colorectal cancer tissue. Scand J Gastroenterol 2009;44:1443–51.
[55] Schnier JB, Nishi K, Gumerlock PH, Gorin FA, Bradbury EM. Glycogen synthesis correlates with androgen-dependent growth arrest in prostate cancer. BMC Urol 2005;5:6.
[56] Charafe-Jauffret E, Monville F, Bertucci F, Esterni B, Ginestier C, Finetti P, et al. Moesin expression is a marker of basal breast carcinomas. Int J Cancer 2007;121:1779–85.
[57] Belbin TJ, Singh B, Smith RV, Socci ND, Wreesmann VB. Molecular profiling of tumor progression in head and neck cancer. Arch Otolaryngol Head Neck Surg 2005;131:10–8.
[58] Kobel M, Gradhand E, Zeng K, Schmitt WD, Kriese K, Lantzsch T. Ezrin promotes ovarian carcinoma cell invasion and its retained expression predicts poor prognosis in ovarian carcinoma. Int J Gynecol Pathol 2006;25:121–30.
[59] Bartholow TL, Chandran UR, Becich MJ, Parwani AV. Immunohistochemical staining of radixin and moesin in prostatic adenocarcinoma. BMC Clin Pathol 2011;11:1.
[60] Cai XW, Shedden K, Ao X, Davis M, Fu XL, Lawrence TS, et al. Plasma proteomics analysis may identify new markers for radiation-induced lung toxicity patients with non-small-cell lung cancer. Int J Radiat Oncol Biol Phys 2010;77:867–76.
[61] Harermann JK, Roblick UJ, Luke BT, Prieto DA, Finlay WJJ, Podust VN. Increased serum levels of complement C3a anaphylatoxin indicate the presence of colorectal tumors. Gastroenterol 2006;131:1020–9.
[62] Kasapovic J, Pejic S, Stojiljkovic V, Todorovicv A, Radosevic-Jelic L, Saicic ZS, et al. Antioxidant status and lipid peroxidation in the blood of breast cancer patients of different ages after chemotherapy with 5-fluorouracil, doxorubicin and cyclophosphamide. Clin Biochem 2010;43:1287–93.
[63] Roncucci L, Mora E, Mariani F. Myeloperoxidase-positive cell infiltration in colorectal carcinogenesis as indicator of colorectal cancer risk. Cancer Epidemiol Biomark 2008;17:2291–7.
[64] Willis ND, Cox1 TR, Rahman-Casans SF, Smits K, Przyborski SA, Brandt P. Lamin A/C is a risk biomarker in colorectal cancer. PLoS ONE 2008;3:e2988.
[65] Yuan Y, Li W, Li L, Yang X, Gu R, Liu H, et al. Effects of tetrazanbigen on the protein expression in human hepatocellular carcinoma cell line QGY-7701. J Huazhong Univ Sci Technolog Med Sci 2009;29:304–8.
[66] Lam JS, Seligson DB, Yu H, Li A, Eeva M, Pantuck AJ, et al. Flap endonuclease 1 is overexpressed in prostate cancer and is associated with a high Gleason score. BJU Int 2006;98:445–51.
[67] Kucherlapati M, Yang K, Kuraguchi M, Zhao J, Lia M, Heyer J. Haploinsufficiency of flap endonuclease (fen1) leads to rapid tumor progression. Proc Natl Acad Sci USA 2002;99:9924–9.
[68] Mikuriya K, Kuramatsu Y, Ryozawa S, Fujimoto M, Mori S, Oka M, et al. Expression of glycolytic enzymes is increased in pancreatic cancerous tissues as evidenced by proteomic profiling by two-dimensional electrophoresis and liquid chromatography–mass spectrometry/mass spectrometry. Int J Oncol 2007;30:849–55.
[69] Hirakawa H, Shibata K, Nakayama T. Localization of cortactin is associated with colorectal cancer development. Int J Oncol 2009;35:1271–6.
[70] Otsubo T, Iwaya K, Mukai Y, Mizokami Y, Serizawa H, Matsuoka T, et al. Involvement of Arp2/3 complex in the process of colorectal carcinogenesis. Mod Pathol 2004;17:461–7.
[71] Tomonaga T, Matsushita K, Yamaguchi S, Oh-Ishi M, Kodera Y, Maeda T. Identification of altered protein expression and post-translational modifications in primary colorectal cancer by using agarose two-dimensional gel electrophoresis. Clin Cancer Res 2004;10:2007–14.
[72] Kranosov GS, Oparina NY, Hankin SL, Mashkova TD, Ershov AN, Zataepina OG, et al. Identification of proteins with altered expression in colorectal cancer by means of 2D-proteomics. Mol Biol 2009;43:321–8.

[73] Chen G, Gharib TG, Huang CC, Thomas DG, Shedden KA, Taylor JM, et al. Proteomic analysis of lung adenocarcinoma: identification of a highly expressed set of proteins in tumors. Clin Cancer Res 2002;8:2298–305.
[74] Nibbe RK, Markowitz S, Myeroff L, Ewing R, Chance MR. Discovery and scoring of protein interaction subnetworks discriminative of late stage human colon cancer. Mol Cell Proteomics 2009;8:827–45.
[75] Tanaka H, Tsukamoto T, Mizoshita T, Inada K, Ogasawara N, Cao X, et al. Expression of small intestinal and colonic phenotypes in complete intestinal metaplasia of the human stomach. Virchows Arch 2005;447:806–15.
[76] Kummola L, Hamalainen JM, Kivela J, Kivela AJ, Saarnio J, Karttunen T. Expression of a novel carbonic anhydrase, CA XIII, in normal and neoplastic colorectal mucosa. BMC Cancer 2005;5:41.
[77] Mizoshita T, Tsukamoto T, Tanaka H, Takenaka Y, Kato S, Cao X, et al. Colonic and small-intestinal phenotypes in gastric cancers: relationships with clinicopathological findings. Pathol Int 2005;10:611–8.
[78] Kang B, Hao C, Wang H, Zhang J, Xing R, Shao J, et al. Evaluation of hepatic-metastasis risk of colorectal cancer upon the protein signature of PI3K/AKT pathway. J Proteome Res 2008;7:3507–15.
[79] Alfonso P, Nunez A, Gurpide JM, Lombardia L, Sanchez L, Casal JI. Proteomic expression analysis of colorectal cancer by two-dimensional differential gel electrophoresis. Proteomics 2005;5:2602–11.
[80] Cappello F, David S, Rappa F, Bucchieri F, Marasa L, Bartolotta TE. The expression of HSP60 and HSP10 in large bowel carcinomas with lymph node metastase. BMC Cancer 2005;5: 139.
[81] Krasnov GS, Khankin SL, Bukurova YA, Zatsepina OG, Oparina NY, Garbuz DG, et al. Proteomic expression analysis of human colorectal cancer: of soluble overexpressed proteins. Mol Biol 2009;43:562–6.
[82] Rho JR, Roehrl MHA, Wang JY. Tissue proteomics reveals differential and compartment-specific expression of the homologs transgelin and transgelin-2 in lung adenocarcinoma and its stroma. J Proteome Res 2009;8:5610–8.
[83] Zhou J, Mulshine JL, Ro JY, Avis I, Yu R, Lee JJ, et al. Expression of heterogeneous nuclear ribonucleoprotein A2/B1 in bronchial epithelium of chronic smokers. Clin Cancer Res 1998;4:1631–40.
[84] Lee C, Lum JH, Cheung BP, Wong M, Butt YK, Tam MF, et al. Identification of the heterogeneous nuclear ribonucleoprotein A2/B1 as the antigen for the gastrointestinal cancer specific monoclonal antibody MG7. Proteomics 2005;5:1160–6.
[85] Sanders YY, Hammons GJ, Lyn-Cook BD. Increased expression of heterogeneous nuclear ribonucleoprotein A2/B1 (hnRNP) in pancreatic tissue from smokers and pancreatic tumor cells. Cancer Lett 2002;183:215–20.
[86] Ma Y, Peng J, Liu W, Zhang P, Huang L, Gao B. Proteomics identification of desmin as a potential oncofetal diagnostic and prognostic biomarker in colorectal cancer. Mol Cell Proteomics 2009;8:1878–90.
[87] Yeo M, Park HJ, Kim DK, Kim YB, Cheong JY, Lee KJ, et al. Loss of SM22 is a characteristic signature of colon carcinogenesis and its restoration suppresses colon tumorigenicity in vivo and in vitro. Cancer 2010;116:2581–9.
[88] Friedman DB, Hill S, Keller JW, Merchant NB, Levy SE, Coffey RJ, et al. Proteome analysis of human colon cancer by two-dimensional difference gel electrophoresis and mass spectrometry. Proteomics 2004;4:793–811.
[89] Loignon M, Miao W, Hu L, Bier A, Bismar TA, Scrivens PJ, et al. Cul3 overexpression depletes Nrf2 in breast cancer and is associated with sensitivity to carcinogens, to oxidative stress, and to chemotherapy. Mol Can Ther 2009;8: 2432–40.
[90] Lai CC, You JF, Yeh CY, Chen JS, Tang R, Wan JY, et al. Low preoperative serum albumin in colon cancer: a risk factor for poor outcome. Int J Colorectal Dis 2011;26:473–81.